The FCV F4 strain was isolated from a cat with respiratory symptoms in Japan (22).

Preparation of FCV F4. Crandell-Rees feline kidney cells (JCRB9035; Health Science Research Resources Bank, Japan) were grown in a 150-cm^2 flask containing Eagle's minimum essential medium (Sigma-Aldrich, St. Louis, MO) with 5% calf serum (JRH Bioscience Corp., Tokyo, Japan) and virus production serum-free medium with L-glutamine (Invitrogen, Carlsbad, CA). Approximately 10^4 PFU of the virus was added to a monolayer of Crandell-Rees feline kidney cells containing 10 ml of culture medium. The cells were incubated for 3 days at 37°C and were harvested when the cytopathic effect had reached 90%. After three cycles of freezing and thawing, the cell debris were removed by centrifugation and the supernatant was stored at −30°C until use.

Full-length cDNA clones. A plasmid designated pUC19/SaV Mc10 full-length containing a full-length SaV Mc10 genome with the T7 promoter, as well as a plasmid designated as pUC19/SaV Mc10 full-C1171A/ORF1 encoding a ^{1169}GDCG^{1172}-to-GDAG mutation in the protease, were expressed as previously described (29).

The FCV F4 genomic RNA was purified from the culture medium by the QIAamp viral RNA mini kit (QIAGEN, Hilden, Germany). FCV F4 cDNA was synthesized as previously described (16). The 5′ fragment corresponding to nucleotides (nt) 1 to 3785 was amplified with the sense primer 5′-GTAAAAG AAATTTGAGACAATGTCTC-3′ and the antisense primer 5′-GTTTACAAA CTAATCCCTTGTAGC-3′. The middle fragment corresponding to nt 2990 to 6971 was amplified with the sense primer 5′-AATGCCAACAGAAAGCTTG A-3′ and the antisense primer 5′-AGCACGCTAATGCGCACTAC-3′. The 3′ fragment corresponding to nt 6952 to 7681 was amplified with the sense primer 5′-GTAGTGCGCATTAGCGTGC-3′ and the antisense primer 5′-CCCTGGG GTTAGACGCAAATGC-3′. These three fragments were cloned into the pCR-BluntII-Topo vector (Invitrogen), and the resulting constructs were designated FCV F4 5′/Topo, FCV F4 middle/Topo, and FCV F4 3′/Topo, respectively. Several amplification and cloning steps were performed to yield a full-length construct with a T7 RNA polymerase promoter at the 5′ end and both a hepatitis D virus (HDV) ribozyme and a T7 terminator at the 3′ end, as described previously (15). To add the HDV ribozyme and the T7 terminator at the 3′ end of the FCV F4 genome, the region from nt 6952 to 7681 was reamplified from the clone 3′/Topo with a sense primer (5′-GTAGTGCGCATTAGCGTGC-3′) and an antisense primer (5′-GAGGTGGAGATGCCATGCCGACCCT$_{30}$CCCTGG GGTTAGACGCAAATGC-3′). HDV ribozyme and T7 terminator sequences were amplified from the pT7HCV09Luc plasmid (45) with a sense primer (5′-GGGTCGGCATGGCATCTCCACCTC-3′) and an antisense primer (5′-GAA CTAGTGGATCCGAGCTCAGATCTCCTTTCAGCAAAAAACCCCTCAA G-3′) that included a BglII site (underlined) and a SacI site (double underlined). These DNA fragments were joined by a primerless PCR as previously described (15), and the amplified fragment corresponding to nt 6952 to 7681 was purified from the gel by using the QIAGel extraction kit (QIAGEN). This DNA fragment was designated FCV F4 6952-7681 polyA-Rz-T7 term. Following these experiments, the FCV F4 region from nt 2990 to 6971 was reamplified with the sense primer 5′-AATGCCAACAGAAAGCTTGA-3′ and the antisense primer 5′-A GCACGCTAATGCGCACTAC-3′. The amplified DNA fragment was joined with 6952-7681 polyA-Rz-T7 term in a primerless PCR. The joined amplified fragment was purified and cloned into the pCR-BluntII-Topo vector, and the construct was designated FCV F4 2990-7681 polyA-Rz-T7 term/Topo. This plasmid was digested with KpnI and SacI (New England Biolabs, Beverly, MA), and the insert was cloned into a pUC19 vector (Toyobo, Osaka, Japan) which was previously digested with KpnI and SacI. The resultant plasmid was designated FCV F4 middle + 3′ polyA-Rz-T7 term/pUC19. Finally, the FCV F4 5′ region corresponding to nt 1 to 3780 was reamplified from FCV F4 5′/Topo with a sense primer (5′-CAGGGGCCCGTCGACCTGGTAATACGACTCACTATAGTAAA AGAAATTTGAGACAATGTC-3′) that included a SalI site (underlined) and a T7 RNA polymerase promoter sequence (bold) and an antisense primer (5′-T TGGGCCATGCAGGTGAGCG-3′). The amplified DNA was purified and digested with SalI and KpnI (New England Biolabs) and cloned into SalI- and KpnI-digested middle + 3′ polyA-Rz-T7 term/pUC19. The resultant plasmid was designated FCV F4 T7-GG full-length-Rz-T7 term/pUC19 ver2 (pUC19/FCV F4 full-length). Sequence analysis confirmed that the cloned genome corresponded to the consensus sequence of FCV F4 (GenBank accession number D31836), with the exception of a silent mutation (T to C) at the nucleotide position 4075.

Site-directed mutagenesis. Site-directed mutagenesis was performed using the GeneTailor site-directed mutagenesis system (Invitrogen), with pUC19/SaV Mc10 full-length (29) and pUC19/FCV F4 full-length as the templates. The site-directed mutagenesis primers are listed in Table 1. The resulting nine SaV Mc10 full-length mutant cDNA clones were designated as follows: pUC19/SaV Mc10 full-H1069A/ORF1 (where the H at amino acid [aa] residue 1069 in the ORF1 product is changed to A), pUC19/SaV Mc10 full-H1075A/ORF1, pUC19/SaV Mc10 full-H1086A/ORF1, pUC19/SaV Mc10 full-E1107A/ORF1, pUC19/SaV Mc10 full-H1120A/ORF1, pUC19/SaV Mc10 full-H1136A/ORF1, pUC19/SaV Mc10 full-E1143A/ORF1, pUC19/SaV Mc10 full-E1147A/ORF1, and pUC19/SaV Mc10 full-H1186A/ORF1. Similarly, 12 FCV F4 full-length mutant cDNA clones were constructed: pUC19/FCV F4 full-H1079A/ORF1, pUC19/FCV F4 full-H1093A/ORF1, pUC19/FCV F4 full-H1099A/ORF1, pUC19/FCV F4 full-H1102A/ORF1, pUC19/FCV F4 full-H1110A/ORF1, pUC19/FCV F4 full-E1121A/ORF1, pUC19/FCV F4 full-D1125A/ORF1, pUC19/FCV F4 full-E1131A/ORF1, pUC19/FCV F4 full-D1155A/ORF1, pUC19/FCV F4 full-E1164A/ORF1, pUC19/FCV F4 full-C1193A/ORF1, and pUC19/FCV F4 full-H1208A/ORF1. All of these full-length clones were verified by sequencing analysis to confirm that there were no additional mutations.

TABLE 1. Oligonucleotides used for the site-directed mutagenesis

Amino acid change[a]	Nucleotide sequence (5′–3′)[b]
SaV polyprotein	
H1069A	CACATCTGGGATGATgccATTGGTATTATTG
H1075A	GATTATTATGGTTTTgccATGTTTAATGTGTG
H1086A	GTTTTCAAGTTACAgccGTGGCCTCTGGTCTT
E1107A	CAGTAATACCAAGGGTgccAGTACCTGGTGAAC
H1120A	TTTGGTCACTTGCCCgccTACCATATGGTATG
H1136A	CTACTACTCGGCGCCTAgccCCTTGCACCAGT
E1143A	GTCACCACGCTTGCGgcgGAAACGTATGAG
E1147A	GCGGAAGGGAACGTATgcgACACCCAATATCAGG
H1186A	CGTTTGTTCGGATCTGgccGCGCCACATCTCAC
FCV polyprotein	
C1193A	ACTCACCCTTGGAGATgccGGTTTCCCTTATATTGGATTAT
H1079A	GGGCCTTCACTAAATTTgccAAAAATGCCATTTAATCAG
H1093A	GATGTGTGTGGAAGAgccAAGGTTACTACATGTCCAC
H1099A	CACAAGGTTACTTGGTgccATGGTTATGGGTTTATG
H1102A	GTTTATTGGTTCCACATGGTgctTGGGTTTATTGGTTTG
H1110A	TATGCTTCTGTGGCAgccGTGGTGAAAGGTGATTCCTAT
E1121A	TATTCCTATTTCTTTGGTgccAATTTTATGTAAAAACC
D1125A	GGTAAAGGATCTTTgccGTAAAACCCAATGGTTAATTCTG
E1131A	GTAAAAACCAATGGTgccTTCTGTTGTTTCGAAGCACT
D1155A	GAAAAGCAAGTCTTgccCCATTGGGTTCGCCAGTTG
E1164A	TGCGGGTCGCCATTTGAACAgcgGTGAAACCAAAGGCCTATAC
H1208A	AGATTTATCGTCTTAgccACTGGATCTGGTGGACCCAAA

[a] Amino acids are shown in the one-letter code. Letters before the numbers indicate the original amino acid residues, and letters after the numbers indicate the mutant amino acid residues.

[b] Only the positive-sense oligonucleotide sequences are shown. The codons corresponding to the changed amino acids are indicated as lowercase letters.

In vitro coupled transcription-translation assay. For an in vitro coupled transcription-translation, linear DNA fragments containing the T7 promoter were generated by PCR with 100 ng of pUC19/SaV Mc10 full-length (29) and nine full-length mutant cDNA clones. DNA fragments corresponding to the entire SaV Mc10 ORF1-encoded region, aa 1 to 2278, were generated with the forward primer SaV Mc10-1F and the antisense primer SaV Mc10-2278R (Table 2). The C-terminally truncated SaV Mc10 ORF1-encoded mutant forms corresponding to the regions from aa 1 to 1246, 1 to 1240, 1 to 1234, 1 to 1229, 1 to 1223, 1 to 1218, 1 to 1212, 1 to 1206, 1 to 1205, 1 to 1204, 1 to 1203, 1 to 1202, 1 to 1201, 1 to 1200, and 1 to 1194 were generated with the forward primer SaV Mc10-1F and the antisense primers SaV Mc10-1246R, SaV Mc10-1240R, SaV Mc10-1234R, SaV Mc10-1229R, SaV Mc10-1223R, SaV Mc10-1218R, SaV Mc10-1212R, SaV Mc10-1206R, SaV Mc10-1205R, SaV Mc10-1204R, SaV Mc10-1203R, SaV Mc10-1202R, SaV Mc10-1201R, SaV Mc10-1200R, and SaV Mc10-1194R (Table 2). Similarly, linear DNA fragments corresponding to the entire and the C-terminally truncated FCV F4 ORF1-encoded regions and containing the T7 promoter were generated by PCR with 100 ng of the pUC19/FCV F4 full-length clone or with 12 full-length mutant cDNA clones. DNA fragments corresponding to the entire FCV ORF1-encoded region, aa 1 to 1763, were generated with the forward primer FCV F4-1F and the antisense primer FCV F4-1763R (Table 2). The truncated FCV F4 ORF1 mutant forms corresponding to the regions from aa 1 to 1419, 1 to 1345, 1 to 1267, 1 to 1245, 1 to 1240, 1 to 1235, 1 to 1230, 1 to 1225, 1 to 1224, and 1 to 1223 were generated with the forward primer FCV F4-1F and the antisense primers FCV F4-1419R, FCV F4-1345R, FCV F4-1267R, FCV F4-1245R, FCV F4-1240R, FCV F4-1235R, FCV F4-1230R, FCV F4-1225R, FCV F4-1224R, and FCV F4-1223R (Table 2).

In vitro T7 polymerase coupled transcription-translation was performed by using the TNT T7 Quick for PCR DNA kit (Promega, Madison, WI) as previ-

TABLE 2. PCR primers to prepare templates for in vitro transcription-translation

Primer name[a]	Sequence (5′–3′)
SaV primers	
SaV Mc10-1F	GCTTCCAAGCCATTCTACCCAATAGAG
SaV Mc10-2278R	TTCTAAGAACCTAACGGCCCGG
SaV Mc10-1246R	TTCTCCTTCCACAGGGTTGGGC
SaV Mc10-1240R	GGGCCATGCAGGTGAGCGGTG
SaV Mc10-1234R	GTGGTAACGAGTCCCCGTGG
SaV Mc10-1229R	CGTGGGCATGCCGCCACAGTC
SaV Mc10-1223R	GTCGGGGCCTCGAACCACTGGTAG
SaV Mc10-1218R	CACTGGTAGACCCTTCCAAGC
SaV Mc10-1212R	AGCAAAAGCATTCTCCAC
SaV Mc10-1206R	CTTGGATGTTTTAGTCAC
SaV Mc10-1205R	GGATGTTTTAGTCACTCGCTGAGCAAGCTTGG
SaV Mc10-1204R	TGTTTTAGTCACTCGCTGAGCAAGCTTGG
SaV Mc10-1203R	TTTAGTCACTCGCTGAGCAAGCTTGG
SaV Mc10-1202R	AGTCACTCGCTGAGCAAGCTTGG
SaV Mc10-1201R	CACTCGCTGAGCAAGCTTGG
SaV Mc10-1200R	TCGCTGAGCAAGCTTGG
SaV Mc10-1194R	CTCACTGAATGACAATTTGGTG
FCV primers	
FCV F4-1F	TCTCAAACTCTGAGCTTCGTG
FCV F4-1763R	TCAAACTTCGAACACATCACAGTG
FCV F4-1419R	CTCTTGCACCTTCTCAATGGG
FCV F4-1345R	TTCAGAGGAGATGTTCATGGG
FCV F4-1267R	AGTGCCTTTTGGTATGATCC
FCV F4-1245R	AGGTTTTGTTTCATCATACTT
FCV F4-1240R	ATACTTTTGAGGGGTTACAGATTTG
FCV F4-1235R	TACAGATTTGTTTTTCATATCAATG
FCV F4-1230R	CATATCAATGTGGATGTAGGGTAC
FCV F4-1225R	GTAGGGTACCACCAATTTTGCGCTTGG
FCV F4-1224R	GGGTACCACCAATTTTGCGCTTGG
FCV F4-1223R	TACCACCAATTTTGCGCTTGG

[a] Primer names ending in F are those of forward primers that include the sequence 5′-GGATCCTAATACGACTCACTATAGGGAACAGCCACCAT G-3′ with the T7 promoter (underlined) and an additional start codon (bold) at the 5′ ends. Primer names ending in R are those of reverse primers (5′-T_{30}TTA-3′) that include poly(A) with a stop codon (bold) at the 5′ ends.

ously described, except that a 25-μl reaction volume and 3 h of incubation were used. The translation products were separated by sodium dodecyl sulfate-polyacrylamide gel electrophoresis (SDS-PAGE), and the radiolabeled proteins were detected as previously described (29, 30).

Nucleotide and amino acid sequence analyses. Nucleotide sequence analysis was performed with the BigDye Terminator (version 3.1) cycle sequencing ready reaction kit (Applied Biosystems, Tokyo, Japan) and an automated sequencer (genetic analyzer 3130; Applied Biosystems). Nucleotide sequences were assembled with the program Sequencher, version 4.2.2 (Gene Codes Corp., Ann Arbor, MI). Nucleotide and amino acid sequences were analyzed with GENETYX Mac software, version 12.2.6 (Genetyx Corp., Tokyo, Japan).

Molecular modeling of SaV, FCV, and RHDV 3C-like proteases. The crystal structure of the NoV 3C-like protease (Protein Data Bank [PDB] code, 1WQS) (27) at a resolution of 2.80 Å was used as the template for the molecular modeling of the SaV, FCV, and RHDV 3C-like proteases. To minimize misalignments of the target and template sequences, multiple-sequence alignments of 3C cysteine proteases, including rhinovirus 3C protease (PDB code, 1CQQ) (23), poliovirus 3C protease (PDB code, 1LIN) (26), and hepatitis A virus 3C protease (PDB code, 1QA7) (3), were used. The alignments were generated using MOE-Align in the Molecular Operating Environment (MOE) package (Chemical Computing Group, Inc., Montreal, Quebec, Canada). 3-D models of SaV Mc10, FCV F4, and RHDV FRG 3C-like proteases were constructed by the homology modeling technique using MOE-Homology in the MOE package as described previously (17, 18). The 3-D structures were thermodynamically optimized by energy minimization with the MOE package and an AMBER99 force field (31). A physically unacceptable local structure of the optimized 3-D model was further refined on the basis of Ramachandran plot evaluation using the MOE package. The quality of the models was assessed using the 3-D-structure evaluation program Verify3D (6, 47).

Strains for amino acid sequence alignments. The 16 SaV strains used for amino acid sequence alignments are as follows, with the nucleotide sequence accession numbers for the corresponding nucleotide regions given in parentheses: Mc114 (AY237422), Manchester (X86560), Dresden (AY694184), N21 (AY237423), Nongkhai50 (AY646853), Chantaburi74 (AY646854), Mc10 (AY237420), Bristol (AJ249939), C12 (AY603425), Mc2 (AY237419), SK15 (AY646855), PEC Cowden (AF182760), PEC LL14 (NC 000940), Ehime1107 (DQ058829), Sw278 (DQ125333), and NK24 (AY646856). The 13 FCV strains used for amino acid sequence alignments are as follows, with the nucleotide sequence accession numbers for the corresponding nucleotide regions given in parentheses: F4 (D31836), F65 (AF109465), 2024 (AF479590), Urbana (L40021), F9 (M86379), CFI/68 (U13992), DD/2006/GE (DQ424892), UTCV-NH1 (AY560113), UTCV-NH2 (AY560114), UTCV-NH3 (AY560115), UTCV-H1 (AY560116), UTCV-H2 (AY560117), and USDA (AY560118).

RESULTS AND DISCUSSION

Identification of the C terminus of the SaV Mc10 3C-like protease. The SaV protease-polymerase (Pro-Pol) is a stable product in both an in vitro translation system and an *Escherichia coli* expression system (28–30). Chang et al. also identified Pro-Pol as a stable product in porcine SaV-infected cells (7). Recently, we identified A^{1056} and E^{1722} as the N and C termini, respectively, of the SaV Mc10 Pro-Pol (Fig. 1A) (28, 30). To define the amino acid residues essential for protease activity, full-length forms and a series of 15 C-terminally truncated forms of the ORF1 polyprotein were expressed in an in vitro transcription-translation system (Fig. 1B; Table 1). The expression was carried out with both wild-type (Pro^{w}) and C1171A mutant (Pro^{mut}) forms of the protease, and the latter were used as a negative control for the proteolytic processing as previously described (29, 30).

At least seven proteins, p28, p32, p35 (NTPase), p46 (p32-VPg), p60 (VP1), p66 (p28-NTPase), and p120 (p32-VPg-Pro-Pol), were detected by direct SDS-PAGE analysis when the ORF1 Pro^{w} form corresponding to aa 1 to 2278 was expressed, and a major 250-kDa product (p250) corresponding to the ORF1 polyprotein appeared when the full-length ORF1 Pro^{mut} form was expressed (29). If the functional protease domain is eliminated, the cleavage patterns of the Pro^{w} forms should be significantly changed. We first analyzed two C-terminally truncated forms corresponding to aa 1 to 1246 and aa 1 to 1194. The proteolytic cleavage occurred in aa 1 to 1246 but not in aa 1 to 1194 (Fig. 1B). The translated product size of the Pro^{w} form of aa 1 to 1194 was identical to that of the Pro^{mut} form of aa 1 to 1194 (Fig. 1B), demonstrating that the C terminus of the functional protease domain is positioned downstream of aa 1194. Next, eight C-terminally truncated forms of the ORF1 polyprotein, aa 1 to 1240, 1 to 1234, 1 to 1229, 1 to 1223, 1 to 1218, 1 to 1212, 1 to 1206, and 1 to 1200, were expressed and analyzed. The proteolytic cleavage occurred efficiently in the Pro^{w} forms of the C-terminally truncated ORF1 polyproteins with aa 1 to 1240, 1 to 1234, 1 to 1229, 1 to 1223, 1 to 1218, 1 to 1212, and 1 to 1206 but not in the form with aa 1 to 1200 (Fig. 1B), demonstrating that the C terminus of the functional protease domain is positioned between aa 1200 and 1206. Finally, we expressed and analyzed five C-terminally truncated forms of the ORF1 polyprotein, aa 1 to 1205, 1 to 1204, 1 to 1203, 1 to 1202, and 1 to 1201. The cleavage occurred efficiently in the Pro^{w} forms of these C-terminally truncated ORF1 polyproteins (Fig. 1B). These results indicated that the C terminus of the functional protease

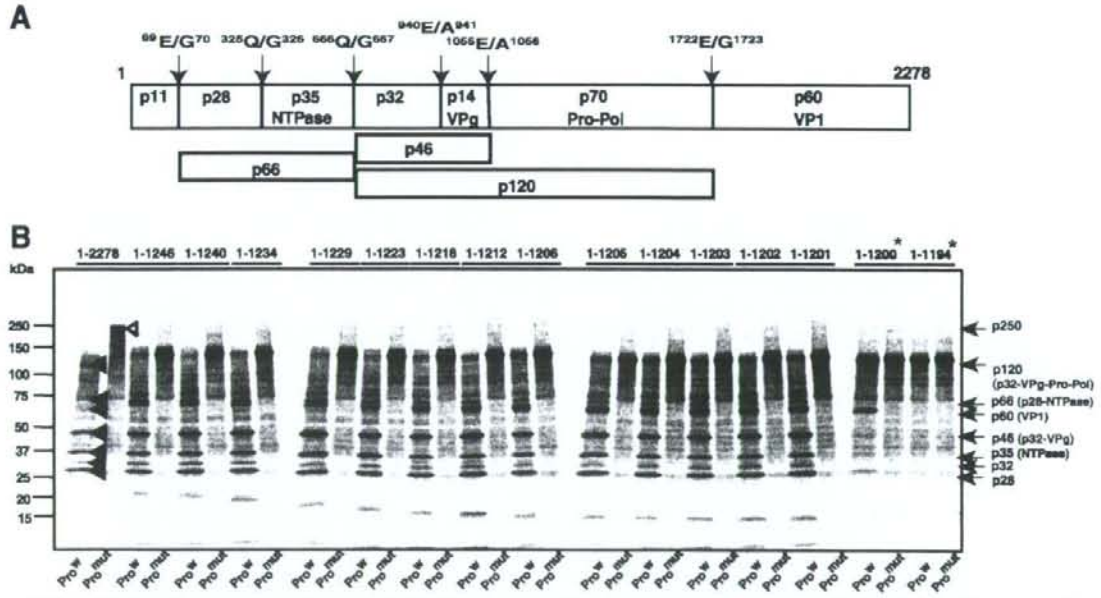

FIG. 1. Identification of the C terminus of the SaV Mc10 protease. (A) Proteolytic cleavage map of the SaV Mc10 ORF1 polyprotein and the processing intermediates (30). (B) SDS-PAGE of in vitro ^{35}S-labeled wild-type (Pro^{w}) and C1171A mutant (Pro^{mut}) forms of the entire ORF1 polyprotein (aa 1 to 2278) and 15 C-terminally truncated polyproteins corresponding to aa 1 to 1246, 1 to 1240, 1 to 1234, 1 to 1229, 1 to 1223, 1 to 1218, 1 to 1212, 1 to 1206, 1 to 1205, 1 to 1204, 1 to 1203, 1 to 1202, 1 to 1201, 1 to 1200, and 1 to 1194. The protein bands corresponding to either the Pro^{w} or Pro^{mut} form of the entire ORF1 polyprotein are indicated by filled and open arrowheads, respectively. The molecular sizes of viral proteins are shown on the right, and size markers are shown on the left. Asterisks indicate two C-terminally truncated forms, corresponding to aa 1 to 1200 and 1 to 1194, which show affected protease activity. Products of approximately 15 to 20 kDa would be the truncated Pro-Pol, released from the truncated ORF1 polyprotein. A 60-kDa product of the C-terminally truncated form corresponding to aa 1 to 1200 was identified as p32-VPg-truncated Pro-Pol.

of SaV Mc10 is V^{1201}, and it seems that the polymerase domain is not important for the protease activity. This amino acid residue was conserved in the 14 human and 2 porcine SaV strains listed in Materials and Methods (data not shown). The Mc10 3C-like protease domain comprises 146 aa (A^{1056} to V^{1201}), similar to the proteases of RHDV (143 aa) and NoV (181 aa) (5, 36).

Identification of the active-site residues of the SaV Mc10 3C-like protease. SaV Mc10 3C-like protease cleaves after the E or Q residue of the specific site in the ORF1 polyprotein (Fig. 1), and the C^{1171} in the GDCG motif was shown to be critical to the protease activity (28–30). Furthermore, the functional SaV Mc10 protease was found to be similar in size to those of RHDV and NoV. These results suggested that the catalytic amino acid residues of the SaV Mc10 protease would also be similar to those of other caliciviruses. In RHDV and NoV, the amino acid residues critical to protease activity have been identified as H^{27}, D^{44}, C^{104}, and H^{119} and H^{30}, E^{54}, C^{139}, and H^{157}, respectively, although it remains controversial whether or not E^{54} has a critical role in NoV protease activity (5, 14, 36, 46). The amino acid essential for the protease activity will definitely be conserved among all SaV strains (at least among human SaV strains) as it is in NoV and RHDV (36) (data not shown). Nine amino acid residues (H^{1069}, H^{1075}, H^{1086}, E^{1107}, H^{1120}, H^{1136}, E^{1143}, E^{1147}, and H^{1186}) within the

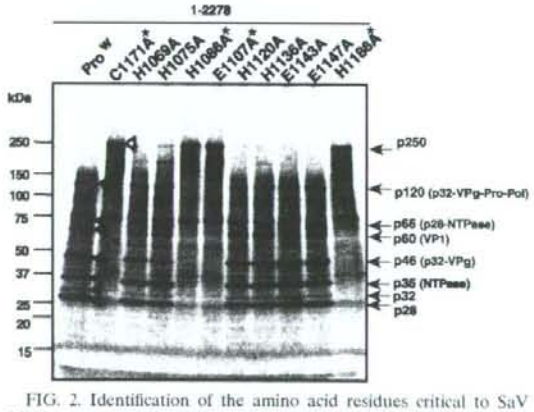

FIG. 2. Identification of the amino acid residues critical to SaV Mc10 protease activity. Shown are the results of SDS-PAGE of in vitro ^{35}S-labeled wild-type (Pro^{w}) and C1171A mutant forms of the entire ORF1 polyprotein (aa 1 to 2278) and nine other mutant forms, the H1069A, H1075A, H1086A, E1107A, H1120A, H1136A, E1143A, E1147A, and H1186A polyproteins. The protein bands corresponding to either the Pro^{w} or C1171A form of the entire ORF1 polyprotein are indicated by filled and open arrowheads, respectively. The molecular sizes of viral proteins are shown on the right, and size markers are shown on the left. Asterisks indicate four mutant forms, the C1171A, H1086A, E1107A, and H1186A polyproteins, which display affected protease activity.

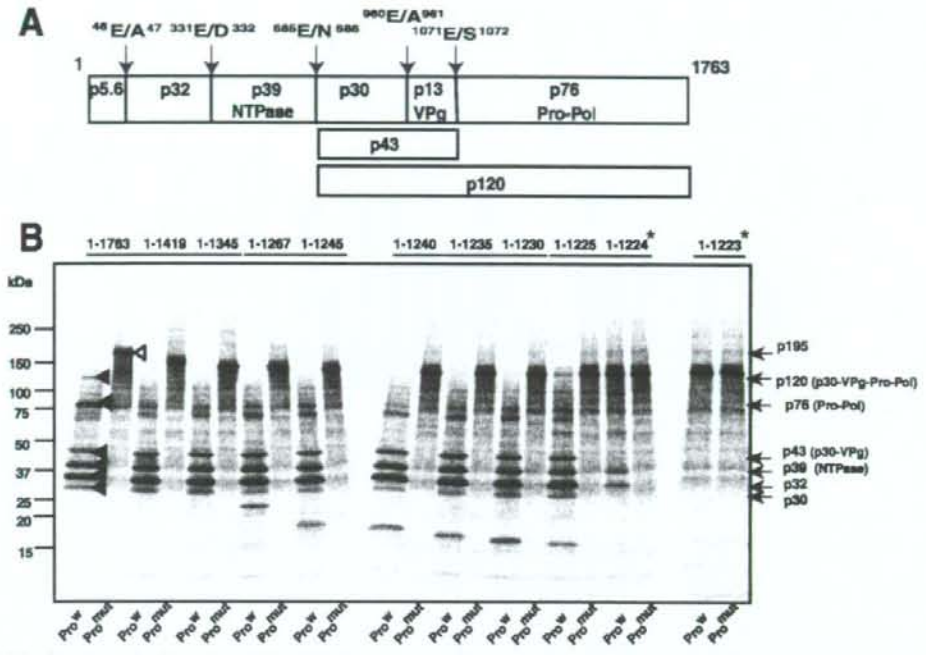

FIG. 3. Identification of the C terminus of the FCV F4 protease. (A) Proteolytic cleavage map of the FCV F4 ORF1 polyprotein and processing intermediates. The locations and designations of the proteins are adopted from the studies by Sosnovtsev et al. (40). (B) SDS-PAGE of in vitro ^{35}S-labeled wild-type (Pro^{w}) and C1193A mutant (Pro^{mut}) forms of the entire ORF1 polyprotein (aa 1 to 1763) and 10 C-terminally truncated polyproteins corresponding to aa 1 to 1419, 1 to 1345, 1 to 1267, 1 to 1245, 1 to 1240, 1 to 1235, 1 to 1230, 1 to 1225, 1 to 1224, and 1 to 1223. The protein bands corresponding to either the Pro^{w} or Pro^{mut} form of the entire ORF1 polyprotein are indicated by filled and open arrowheads, respectively. The molecular sizes of viral proteins are shown on the right, and size markers are shown on the left. Asterisks indicate two C-terminally truncated forms, corresponding to aa 1 to 1224 and 1 to 1223, which display affected protease activity. Products of approximately 15 to 25 kDa would be the truncated Pro-Pol released from the truncated ORF1 polyprotein.

protease domain were selected based on the amino acid alignment of 14 human SaV strains, with one exception: D instead of E^{1147} in a human SaV NK24 strain (data not shown). These nine amino acid residues were changed to A by site-directed mutagenesis (Table 1), and nine mutant forms of the ORF1 polyprotein, the H1069A, H1075A, H1086A, E1107A, H1120A, H1136A, E1143A, E1147A, and H1186A forms, were expressed in an in vitro translation system. Two forms of the ORF1 polyprotein, the full-length Pro^{w} and Pro^{mut} (C1171A) forms, were used as positive and negative controls, respectively (Fig. 2) (29, 30). Three mutant forms of the ORF1 polyprotein, the H1086A, E1107A, and H1186A forms, each produced a major 250-kDa product (Fig. 2), demonstrating that the proteolytic processing of the ORF1 polyprotein was completely blocked with these mutant forms. In contrast, the cleavage products of six mutant forms, the H1069A, H1075A, H1120A, H1136A, E1143A, and E1147A forms, were identical to those of Pro^{w}, although their cleavages were slightly affected (Fig. 2). From these results, we concluded that the amino acid residues critical to SaV Mc10 3C-like protease activity are $H^{1086(31)}$, $E^{1107(52)}$, $C^{1171(116)}$, and $H^{1186(131)}$. The first three of these would form the catalytic triad (general base, anion, and nucleophile, respectively), and the last one would correspond to part of the binding pocket as previously described for other calicivirus proteases (5, 27, 36, 46). Two amino acids, E^{1107} and H^{1186}, essential to the SaV Mc10 protease activity are not conserved in porcine SaV; (i) E^{1107} in Mc10 is D in the PEC LL14 and Cowden strains, and (ii) H^{1186} in Mc10 is Y in the PEC LL14 strain, whereas H^{1186} is conserved in the PEC Cowden strain (data not shown).

Identification of the C terminus of the FCV F4 3C-like protease. The FCV protease-polymerase (Pro-Pol) has been identified as a stable product in both infected cells and an in vitro translation system (12, 40). Sosnovtseva et al. reported that the entire Pro-Pol region is not essential for the autocatalytic polyprotein processing in the Urbana strain in vitro translation system (42). However, the exact C terminus of the functional protease domain has not been determined.

We generated two full-length cDNA clones, pUC19/FCV F4 full-length and pUC19/FCV F4 full-C1193A/ORF1, the latter of which encodes a ^{1191}GDCG^{1194}-to-GDAG mutation in the protease. The expression was carried out with both Pro^{w} and Pro^{mut} (C1193A) forms of the protease, and the latter were used as a negative control for the proteolytic processing. Six major cleavage products, p30, p32, p39 (NTPase), p43 (p30-VPg), p76 (Pro-Pol), and p120 (p30-VPg-Pro-Pol), were detected when the Pro^{w} form corresponding to aa 1 to 1763 was expressed in an in vitro translation system (Fig. 3). These

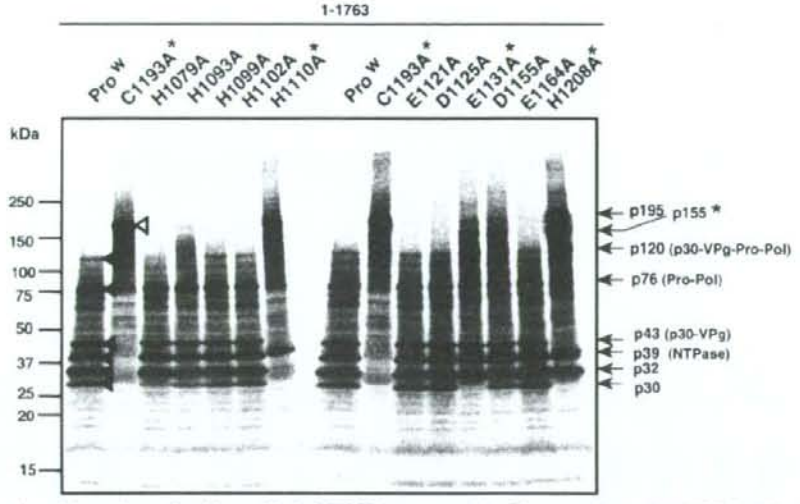

FIG. 4. Identification of the amino acid residues critical to FCV F4 protease activity. Shown are the results of SDS-PAGE of in vitro ^{35}S-labeled wild-type (Pro^{w}) and C1193A mutant forms of the entire ORF1 polyprotein (aa 1 to 1763) and 11 other mutant forms, the H1079A, H1093A, H1099A, H1102A, H1110A, E1121A, D1125A, E1131A, D1155A, E1164A, and H1208A polyproteins. The protein bands corresponding to either the Pro^{w} or C1193A form of the entire ORF1 polyprotein are indicated by filled and open arrowheads, respectively. The molecular sizes of viral proteins are shown on the right, and size markers are shown on the left. Asterisks indicate four mutant forms, the C1193A, H1110A, E1131A, and H1208A polyproteins, which show affected protease activity. The newly appearing product, p155, also marked with an asterisk, probably corresponds to NTPase-p30-VPg-Pro-Pol.

cleavage products were identical to those of the Urbana strain (40). A major 195-kDa product (p195) corresponding to the ORF1 polyprotein appeared when the Pro^{mut} form was expressed (Fig. 3B), demonstrating that the C^{1193} is critical to the FCV F4 3C-like protease activity, consistent with a previous report (42).

To define the C terminus of the functional protease domain of FCV F4, a series of 10 C-terminally truncated ORF1 polyproteins were expressed in an in vitro translation system (Fig. 3B; Table 1). Both Pro^{w} and Pro^{mut} forms of each of these regions were expressed, and the latter were used as a negative control for the proteolytic processing. Eight C-terminally truncated templates corresponding to aa 1 to 1419, 1 to 1345, 1 to 1267, 1 to 1245, 1 to 1240, 1 to 1235, 1 to 1230, and 1 to 1223 were first expressed and analyzed. The proteolytic cleavage occurred in the Pro^{w} forms of the C-terminally truncated ORF1 polyproteins corresponding to aa 1 to 1419, 1 to 1345, 1 to 1267, 1 to 1245, 1 to 1240, 1 to 1235, and 1 to 1230 but not in that corresponding to aa 1 to 1223. The translated product size of the Pro^{w} form of aa 1 to 1223 was identical to that of the Pro^{mut} form of aa 1 to 1223 (Fig. 3B), demonstrating that the C terminus of the functional protease domain is positioned upstream of aa 1223. Next, we expressed and analyzed two additional C-terminally truncated forms, aa 1 to 1225 and 1 to 1224. The proteolytic cleavage occurred efficiently when the Pro^{w} form of aa 1 to 1225 was expressed, whereas it occurred partially when the Pro^{w} form of aa 1 to 1224 was expressed (Fig. 3B). The C terminus of the functional protease domain for FCV F4 was determined to be Y^{1225}. This amino acid is conserved in 13 FCV strains (data not shown). Although we did not identify the cleavage sites of the FCV F4 ORF1 polyprotein, the cleavage pattern and the sizes of the products were consistent with the results of Sosnovtsev et al. (40). Therefore, the size of the functional protease of FCV F4 would be 154 aa (S^{1072} to Y^{1225}) when the cleavage site of the N terminus of the Urbana strain Pro-Pol is considered (40). The FCV F4 functional protease domain is similar in size to those of other caliciviruses, including SaV.

Identification of the active sites of the FCV F4 3C-like protease. The FCV 3C-like protease cleaves after the E residues of the specific site in the ORF1 polyprotein (Fig. 3A), and the C in the GDCG motif is critical to the protease activity (40–42). The functional FCV F4 protease is similar in size to those of SaV, RHDV, and NoV. Thus, the catalytic amino acid residues of the FCV protease would also be similar to those of SaV, RHDV, and NoV. Therefore, 11 amino acid residues (H^{1079}, H^{1093}, H^{1099}, H^{1102}, H^{1110}, E^{1121}, D^{1125}, E^{1131}, D^{1155}, E^{1164}, and H^{1208}) within the protease domain were selected and were changed to A by site-directed mutagenesis (Table 1).

Eleven mutant forms of the ORF1 polyprotein, the H1079A, H1093A, H1099A, H1102A, H1110A, E1121A, D1125A, E1131A, D1155A, E1164A, and H1208A forms, were expressed in an in vitro translation system. Two forms of ORF1 polyprotein, the full-length Pro^{w} and Pro^{mut} (C1193A) forms, were used as positive and negative controls for the proteolytic processing (Fig. 4). H1110A did significantly affect the ORF1 polyprotein processing, whereas E1131A and H1208A affected the processing partially (Fig. 4). That is, (i) p195, the entire ORF1 polyprotein, was detected when the H1110A form was expressed, (ii) p30 disappeared and p155 (likely the stable intermediate of NTPase-p30-VPg-Pro-Pol) appeared when the E1131A form was expressed, and (iii) p195 and p155 (NTPase-

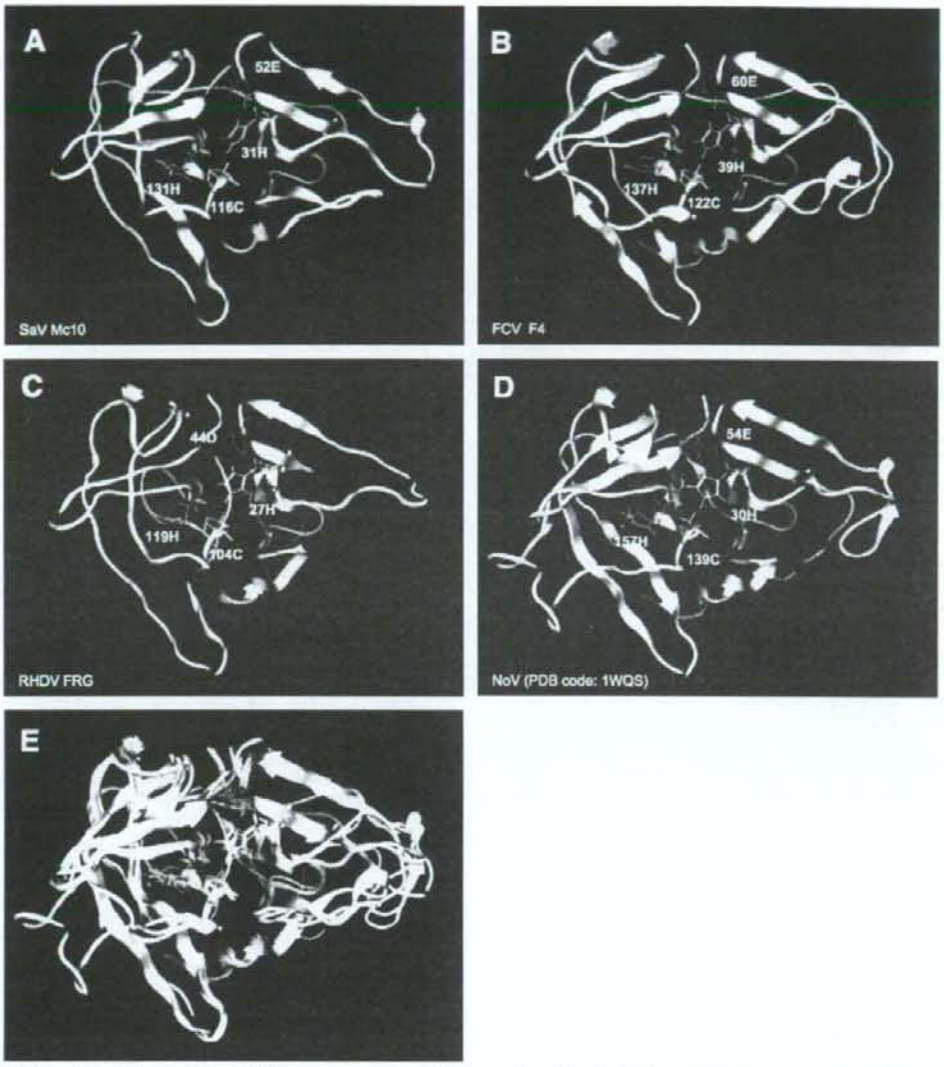

FIG. 5. 3-D models of the calicivirus 3C-like proteases. (A to D) Structural models of calicivirus 3C-like protease domains of the SaV Mc10 (A), FCV F4 (B), and RHDV FRG (C) strains and crystal structure of the NoV Chiba strain protease (27) (D). (E) Superimposition of 3C-like protease structures of the SaV Mc10, FCV F4, RHDV FRG, and NoV Chiba strains. The models were constructed with a homology modeling technique by using programs in the MOE package. Ribbons represent the backbone of the 3C-like protease domain. Side chains of the catalytically important amino acids identified in this study are shown as cyan sticks (H), red sticks (D and E), yellow sticks (C), and green sticks (H).

p30-VPg-Pro-Pol) appeared whereas p43 (p30-VPg) and p30 disappeared when the H1208A form was expressed. Prolonged incubation for up to 16 h did not change the processing patterns of these templates (data not shown). In contrast, the proteolytic processing of the ORF1 polyprotein was barely affected when five mutant forms, the H1099A, H1102A, E1121A, D1125A, and D1155A forms, were expressed (Fig. 4). The p120 (p30-VPg-Pro-Pol) band disappeared when two mutant forms, the H1079A and H1093A forms, were expressed. However, the mutated amino acid residues in these forms are not critical to protease activity, because other cleavage products were produced normally. Therefore, this product would be a precursor intermediate. Combining these results, we concluded that the amino acid residues important to FCV F4 3C-like protease activity are $H^{1110(39)}$, $E^{1131(60)}$, $C^{1193(122)}$, and $H^{1208(137)}$. The former three amino acid residues would form

the catalytic triad, and the last amino acid residue would correspond to a part of the binding pocket as discussed for other calicivirus proteases. A reverse genetics system has been reported for FCV (37, 38, 40), and it would be interesting to evaluate whether the E1131A and H1208A mutant forms are also important in vivo.

Structural modeling of SaV and FCV 3C-like proteases. Processing activities and specificities of the SaV and FCV 3C-like protease were similar when 3D-like RNA-dependent RNA polymerase domains were sequentially deleted (Fig. 1 and 3), strongly suggesting that the structure of the protease active site is self-determined and preserved in the part of the Pro-Pol polypeptide independent of the Pol domain. To obtain structural insights into the roles of the amino acid residues critical to protease activity, 3-D models of the 3C-like protease domains of the SaV Mc10, FCV F4, and RHDV FRG strains were constructed and compared with the X-ray crystal structure of the 3C-like protease of the NoV Chiba strain (27). Despite the low levels of amino acid sequence similarity of proteases among these strains (about 20%), the overall structures were predicted to be similar and to retain structural characteristics seen in the functional protease in general (Fig. 5A to D). The calicivirus proteases consist of N- and C-terminal subdomains, which are separated by a large cleft, probably for substrate binding. H and E in SaV, FCV, and NoV and H and D in RHDV are located along the inner surface of the N-terminal subdomain, whereas C and H in all viruses are located along the inner surface of the C-terminal subdomain. In contrast to the overall similarity, the conformations and configurations of the local structures around the active site are often different among the viruses, suggesting their potential roles in determining protein substrate specificity.

Notably, the superimposition of the calicivirus protease domain structures showed that the thermodynamically favored configurations of the amino acids H, E/D, C, and H are highly conserved (Fig. 5E); the side chains of these amino acids protrude from the main chains at almost identical positions, with very similar configurations along the inner surface of the potential binding cleft for the substrate. The C is a part of the GDCG motif, a conserved and functionally important 3C-like protease motif, and is surrounded closely by other amino acid residues, H, E, and H. The side chain orientations are almost identical to those of the protease. Higher-resolution X-ray crystal structures from distinct NoV strains (46) supported the conservation of the configuration of these catalytic amino acid residues among calicivirus proteases. These findings are consistent with the critical roles of these amino acids in the proteolytic activity and suggest strongly that the H, E, C, and H residues are involved in the formation of a conserved catalytic surface of the SaV and FCV 3C-like proteases.

Conclusions. The functional domains, amino acid residues critical to the proteolytic processing activity, and structural characteristics of SaV and FCV 3C-like proteases were identified. The molecular genetics study showed that the sizes and catalytically important amino acids of the SaV and FCV proteases are similar to those of RHDV and NoV proteases. The computer-assisted structural study strongly suggested that these amino acids are involved in the formation of a conserved catalytic surface of the calicivirus 3C-like protease. In this study, we studied both primary and 3-D structures of SaV and FCV proteases, which are mutually closely related subjects and should be understood in concert. In collaboration with other resources, the data obtained in this study will provide important bases to study the molecular function and inhibitors of calicivirus proteases.

ACKNOWLEDGMENTS

We thank Y. Someya for his critical review of the manuscript.

This work was supported in part by grants for research on emerging and reemerging infectious diseases, as well as food safety, from the Ministry of Health, Labor, and Welfare of Japan and by a grant from the Japan Health Science Foundation for Research on Health Sciences Focusing on Drug Innovation.

REFERENCES

1. **Asanaka, M., R. L. Atmar, V. Ruvolo, S. E. Crawford, F. H. Neill, and M. K. Estes.** 2005. Replication and packaging of Norwalk virus RNA in cultured mammalian cells. Proc. Natl. Acad. Sci. USA **102:**10327–10332.
2. **Belliot, G., S. V. Sosnovtsev, T. Mitra, C. Hammer, M. Garfield, and K. Y. Green.** 2003. In vitro proteolytic processing of the MD145 norovirus ORF1 nonstructural polyprotein yields stable precursors and products similar to those detected in calicivirus-infected cells. J. Virol. **77:**10957–10974.
3. **Bergmann, E. M., M. M. Cherney, J. McKendrick, S. Frormann, C. Luo, B. A. Malcolm, J. C. Vederas, and M. N. James.** 1999. Crystal structure of an inhibitor complex of the 3C proteinase from hepatitis A virus (HAV) and implications for the polyprotein processing in HAV. Virology **265:**153–163.
4. **Blakeney, S. J., A. Cahill, and P. A. Reilly.** 2003. Processing of Norwalk virus nonstructural proteins by a 3C-like cysteine proteinase. Virology **308:**216–224.
5. **Boniotti, B., C. Wirblich, M. Sibilia, G. Meyers, H. J. Thiel, and C. Rossi.** 1994. Identification and characterization of a 3C-like protease from rabbit hemorrhagic disease virus, a calicivirus. J. Virol. **68:**6487–6495.
6. **Bowie, J. U., R. Luthy, and D. Eisenberg.** 1991. A method to identify protein sequences that fold into a known three-dimensional structure. Science **253:**164–170.
7. **Chang, K. O., S. S. Sosnovtsev, G. Belliot, Q. Wang, L. J. Saif, and K. Y. Green.** 2005. Reverse genetics system for porcine enteric calicivirus, a prototype sapovirus in the *Caliciviridae*. J. Virol. **79:**1409–1416.
8. **Chang, K. O., S. V. Sosnovtsev, G. Belliot, A. D. King, and K. Y. Green.** 2006. Stable expression of a Norwalk virus RNA replicon in a human hepatoma cell line. Virology **353:**463–473.
9. **Clarke, I. N., and P. R. Lambden.** 2000. Organization and expression of calicivirus genes. J. Infect. Dis. **181**(Suppl. 2)**:**S309–S316.
10. **Clarke, I. N., and P. R. Lambden.** 1997. The molecular biology of caliciviruses. J. Gen. Virol. **78:**291–301.
11. **Green, K. Y., T. Ando, M. S. Balayan, T. Berke, I. N. Clarke, M. K. Estes, D. O. Matson, S. Nakata, J. D. Neill, M. J. Studdert, and H. J. Thiel.** 2000. Taxonomy of the caliciviruses. J. Infect. Dis. **181**(Suppl. 2)**:**S322–S330.
12. **Green, K. Y., A. Mory, M. H. Fogg, A. Weisberg, G. Belliot, M. Wagner, T. Mitra, E. Ehrenfeld, C. E. Cameron, and S. V. Sosnovtsev.** 2002. Isolation of enzymatically active replication complexes from feline calicivirus-infected cells. J. Virol. **76:**8582–8595.
13. **Hansman, G. S., K. Katayama, N. Maneekarn, S. Peerakome, P. Khamrin, S. Tonusin, S. Okitsu, O. Nishio, N. Takeda, and H. Ushijima.** 2004. Genetic diversity of norovirus and sapovirus in hospitalized infants with sporadic cases of acute gastroenteritis in Chiang Mai, Thailand. J. Clin. Microbiol. **42:**1305–1307.
14. **Hardy, M. E., T. J. Crone, J. E. Brower, and K. Ettayebi.** 2002. Substrate specificity of the Norwalk virus 3C-like proteinase. Virus Res. **89:**29–39.
15. **Katayama, K., G. S. Hansman, T. Oka, S. Ogawa, and N. Takeda.** 2006. Investigation of norovirus replication in a human cell line. Arch. Virol. **151:**1291–1308.
16. **Katayama, K., H. Shirato-Horikoshi, S. Kojima, T. Kageyama, T. Oka, F. Hoshino, S. Fukushi, M. Shinohara, K. Uchida, Y. Suzuki, T. Gojobori, and N. Takeda.** 2002. Phylogenetic analysis of the complete genome of 18 Norwalk-like viruses. Virology **299:**225–239.
17. **Kinomoto, M., R. Appiah-Opong, J. A. Brandful, M. Yokoyama, N. Nii-Trebi, E. Ugly-Kwame, H. Sato, D. Ofori-Adjei, T. Kurata, F. Barre-Sinoussi, T. Sata, and K. Tokunaga.** 2005. HIV-1 proteases from drug-naive West African patients are differentially less susceptible to protease inhibitors. Clin. Infect. Dis. **41:**243–251.
18. **Kinomoto, M., M. Yokoyama, H. Sato, A. Kojima, T. Kurata, K. Ikuta, T. Sata, and K. Tokunaga.** 2005. Amino acid 36 in the human immunodeficiency virus type 1 gp41 ectodomain controls fusogenic activity: implications for the molecular mechanism of viral escape from a fusion inhibitor. J. Virol. **79:**5996–6004.
19. **Konig, M., H. J. Thiel, and G. Meyers.** 1998. Detection of viral proteins after infection of cultured hepatocytes with rabbit hemorrhagic disease virus. J. Virol. **72:**4492–4497.

20. **Liu, B., I. N. Clarke, and P. R. Lambden.** 1996. Polyprotein processing in Southampton virus: identification of 3C-like protease cleavage sites by in vitro mutagenesis. J. Virol. **70:**2605–2610.
21. **Liu, B. L., G. J. Viljoen, I. N. Clarke, and P. R. Lambden.** 1999. Identification of further proteolytic cleavage sites in the Southampton calicivirus polyprotein by expression of the viral protease in E. coli. J. Gen. Virol. **80:**291–296.
22. **Makino, A., M. Shimojima, T. Miyazawa, K. Kato, Y. Tohya, and H. Akashi.** 2006. Junctional adhesion molecule 1 is a functional receptor for feline calicivirus. J. Virol. **80:**4482–4490.
23. **Matthews, D. A., P. S. Dragovich, S. E. Webber, S. A. Fuhrman, A. K. Patick, L. S. Zalman, T. F. Hendrickson, R. A. Love, T. J. Prins, J. T. Marakovits, R. Zhou, J. Tikhe, C. E. Ford, J. W. Meador, R. A. Ferre, E. L. Brown, S. L. Binford, M. A. Brothers, D. M. DeLisle, and S. T. Worland.** 1999. Structure-assisted design of mechanism-based irreversible inhibitors of human rhinovirus 3C protease with potent antiviral activity against multiple rhinovirus serotypes. Proc. Natl. Acad. Sci. USA **96:**11000–11007.
24. **Mayo, M. A.** 2002. A summary of taxonomic changes recently approved by ICTV. Arch. Virol. **147:**1655–1663.
25. **Meyers, G., C. Wirblich, H. J. Thiel, and J. O. Thumfart.** 2000. Rabbit hemorrhagic disease virus: genome organization and polyprotein processing of a calicivirus studied after transient expression of cDNA constructs. Virology **276:**349–363.
26. **Mosimann, S. C., M. M. Cherney, S. Sia, S. Plotch, and M. N. James.** 1997. Refined X-ray crystallographic structure of the poliovirus 3C gene product. J. Mol. Biol. **273:**1032–1047.
27. **Nakamura, K., Y. Someya, T. Kumasaka, G. Ueno, M. Yamamoto, T. Sato, N. Takeda, T. Miyamura, and N. Tanaka.** 2005. A norovirus protease structure provides insights into active and substrate binding site integrity. J. Virol. **79:**13685–13693.
28. **Oka, T., K. Katayama, S. Ogawa, G. S. Hansman, T. Kageyama, T. Miyamura, and N. Takeda.** 2005. Cleavage activity of the sapovirus 3C-like protease in Escherichia coli. Arch. Virol. **150:**2539–2548.
29. **Oka, T., K. Katayama, S. Ogawa, G. S. Hansman, T. Kageyama, H. Ushijima, T. Miyamura, and N. Takeda.** 2005. Proteolytic processing of sapovirus ORF1 polyprotein. J. Virol. **79:**7283–7290.
30. **Oka, T., M. Yamamoto, K. Katayama, G. S. Hansman, S. Ogawa, T. Miyamura, and N. Takeda.** 2006. Identification of the cleavage sites of sapovirus open reading frame 1 polyprotein. J. Gen. Virol. **87:**3329–3338.
31. **Ponder, J. W., and D. A. Case.** 2003. Force fields for protein simulations. Adv. Protein Chem. **66:**27–85.
32. **Seah, E. L., J. A. Marshall, and P. J. Wright.** 1999. Open reading frame 1 of the Norwalk-like virus Camberwell: completion of sequence and expression in mammalian cells. J. Virol. **73:**10531–10535.
33. **Seah, E. L., J. A. Marshall, and P. J. Wright.** 2003. *trans* activity of the norovirus Camberwell proteinase and cleavage of the N-terminal protein encoded by ORF1. J. Virol. **77:**7150–7155.
34. **Someya, Y., N. Takeda, and T. Miyamura.** 2005. Characterization of the norovirus 3C-like protease. Virus Res. **110:**91–97.
35. **Someya, Y., N. Takeda, and T. Miyamura.** 2000. Complete nucleotide sequence of the chiba virus genome and functional expression of the 3C-like protease in Escherichia coli. Virology **278:**490–500.
36. **Someya, Y., N. Takeda, and T. Miyamura.** 2002. Identification of active-site amino acid residues in the Chiba virus 3C-like protease. J. Virol. **76:**5949–5958.
37. **Sosnovtsev, S., and K. Y. Green.** 1995. RNA transcripts derived from a cloned full-length copy of the feline calicivirus genome do not require VpG for infectivity. Virology **210:**383–390.
38. **Sosnovtsev, S. V., G. Belliot, K. O. Chang, O. Onwudiwe, and K. Y. Green.** 2005. Feline calicivirus VP2 is essential for the production of infectious virions. J. Virol. **79:**4012–4024.
39. **Sosnovtsev, S. V., G. Belliot, K. O. Chang, V. G. Prikhodko, L. B. Thackray, C. E. Wobus, S. M. Karst, H. W. Virgin, and K. Y. Green.** 2006. Cleavage map and proteolytic processing of the murine norovirus nonstructural polyprotein in infected cells. J. Virol. **80:**7816–7831.
40. **Sosnovtsev, S. V., M. Garfield, and K. Y. Green.** 2002. Processing map and essential cleavage sites of the nonstructural polyprotein encoded by ORF1 of the feline calicivirus genome. J. Virol. **76:**7060–7072.
41. **Sosnovtsev, S. V., S. A. Sosnovtseva, and K. Y. Green.** 1998. Cleavage of the feline calicivirus capsid precursor is mediated by a virus-encoded proteinase. J. Virol. **72:**3051–3059.
42. **Sosnovtseva, S. A., S. V. Sosnovtsev, and K. Y. Green.** 1999. Mapping of the feline calicivirus proteinase responsible for autocatalytic processing of the nonstructural polyprotein and identification of a stable proteinase-polymerase precursor protein. J. Virol. **73:**6626–6633.
43. **Wei, L., J. S. Huhn, A. Mory, H. B. Pathak, S. V. Sosnovtsev, K. Y. Green, and C. E. Cameron.** 2001. Proteinase-polymerase precursor as the active form of feline calicivirus RNA-dependent RNA polymerase. J. Virol. **75:**1211–1219.
44. **Wirblich, C., H. J. Thiel, and G. Meyers.** 1996. Genetic map of the calicivirus rabbit hemorrhagic disease virus as deduced from in vitro translation studies. J. Virol. **70:**7974–7983.
45. **Yap, C. C., K. Ishii, H. Aizaki, H. Tani, Y. Aoki, Y. Ueda, Y. Matsuura, and T. Miyamura.** 1998. Expression of target genes by coinfection with replication-deficient viral vectors. J. Gen. Virol. **79:**1879–1888.
46. **Zeitler, C. E., M. K. Estes, and B. V. Venkataram Prasad.** 2006. X-ray crystallographic structure of the Norwalk virus protease at 1.5-A resolution. J. Virol. **80:**5050–5058.
47. **Zhang, K. Y., and D. Eisenberg.** 1994. The three-dimensional profile method using residue preference as a continuous function of residue environment. Protein Sci. **3:**687–695.

Sapovirus in Water, Japan

Grant S. Hansman,* Daisuke Sano,† You Ueki,‡ Takahiro Imai,† Tomoichiro Oka,* Kazuhiko Katayama,* Naokazu Takeda,* and Tatsuo Omura†

Sapoviruses are etiologic agents of human gastroenteritis. We detected sapovirus in untreated wastewater, treated wastewater, and a river in Japan. A total of 7 of 69 water samples were positive by reverse transcription–PCR. Phylogenetic analysis of the viral capsid gene grouped these strains into 4 genetic clusters.

The family *Caliciviridae* contains 4 genera, *Sapovirus*, *Norovirus*, *Lagovirus*, and *Vesivirus*, which include sapovirus (SaV), norovirus (NoV), rabbit hemorrhagic disease virus, and feline calicivirus strains, respectively. SaV and NoV are agents of human gastroenteritis. The most widely used method of detection is reverse transcription–PCR (RT-PCR), which has a high sensitivity and can also be used for genetic analysis. Only a limited number of SaV studies have been conducted, although most studies have shown that SaV infections are more frequent in young children than in adults and that nearly all children are infected by 5 years of age.

NoVs have been detected in oysters (and other shellfish), water from drinking fountains, ice, and community drinking water (*1–4*). Environmental studies of SaV have not been conducted. SaV strains can be divided into 5 genogroups (GI–GV), among which GI, GII, GIV, and GV infect humans; GIII infects porcine species. Phylogenetic studies have also designated SaV clusters or genotypes to further describe strains that differ by ≈10% in nucleotide or amino acid sequences. The purpose of this study was to identify and describe SaV strains in environmental samples, namely, untreated wastewater, treated wastewater, a river, and seawater, in Japan.

The Study

Water samples were obtained at different locations once a month in Miyagi Prefecture, Japan, from March 14, 2004, through February 16, 2005 (*5*). A total of 69 samples were obtained, which included 12 untreated wastewater samples, 12 treated wastewater samples, 23 river samples (2 different locations), and 22 seawater samples (2 different locations) (Figure 1). Untreated wastewater and treated wastewater were obtained from a wastewater treatment plant that processes domestic wastewater from residents living in a nearby city (Matsushima City). The treated wastewater is chlorinated at the wastewater treatment plant and then discharged into the Takagi River. The river runs directly into Matsushima Bay and then into the Pacific Ocean. River water was obtained from 2 locations upstream from the wastewater treatment plant, and seawater was obtained from 2 locations outside Matsushima Bay in the Pacific Ocean.

The methods of viral concentration were different for each location, as previously described (*5*). For untreated wastewater, 1 L was centrifuged for 15 min at 9,000 × *g* and concentrated with polyethylene glycol (resuspended in 4 mL distilled water). For treated wastewater and river water, 1 L was directly concentrated with polyethylene glycol. For seawater, 10 L was filtered, viruses were absorbed to a filter (type HA negatively charged membrane with a 0.45-μm pore size, Nihon Millipore, Tokyo, Japan) and eluted in 40 mL alkali buffer, and 40 mL buffer was further concentrated by ultracentrifugation to give a final volume of 500 μL (*6*).

RNA was extracted as previously described (*7*). Nested RT-PCR was used to detect all human genogroups (*8*). For the first PCR, primers F13, F14, R13, and R14 were used. For the nested PCR, primers F22 and R2 were used. All RT-PCR products were analyzed by electrophoresis on 2% agarose gels and visualized by staining with ethidium bromide. RT-PCR products were excised from

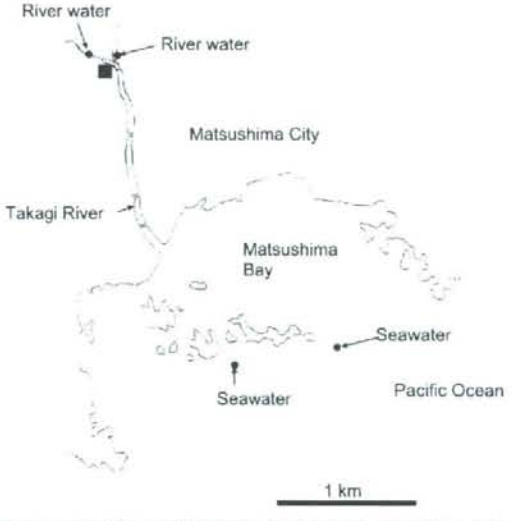

Figure 1. Locations in Miyagi Prefecture, Japan, from which water was isolated. The solid square shows the location of the wastewater treatment plant (sampling site of untreated and treated wastewater).

*National Institute of Infectious Diseases, Tokyo, Japan; †Tohoku University, Sendai, Japan; and ‡Miyagi Prefectural Institute of Public Health and Environment, Sendai, Japan

the gel and purified using the QIAquick gel extraction kit (QIAGEN, Hilden, Germany). Nucleotide sequences were determined with the terminator cycle sequence kit (version 3.1) and the ABI 3130 Avant sequencer (PerkinElmer Biosystems, Wellesley, MA, USA). Sequences were aligned with Clustal X (*9*), and distances were calculated by using the Kimura 2-parameter method as previously described (*10*). Nucleotide sequence data from this study have been deposited in GenBank under accession nos. DQ915088–DQ915094.

SaV was detected in 7 (10%) of 69 concentrated water samples. Negative controls were included in the RT-PCR and showed negative results (data not shown). Genetic analysis of the positive samples showed 4 distinct genetic clusters, which included 3 GI clusters and 1 GV cluster (Figure 2). Three GI sequences were identical (strains 16, 24, and 42), 2 of which were obtained from treated wastewater 3 months apart (strains 24 and 42), and 1 was obtained from the river water (strain 16). The other 2 GI sequences grouped into 2 different clusters (strains 29 and 64) and were isolated from untreated wastewater. The 2 GV sequences were identical (strains 5 and 6). These 2

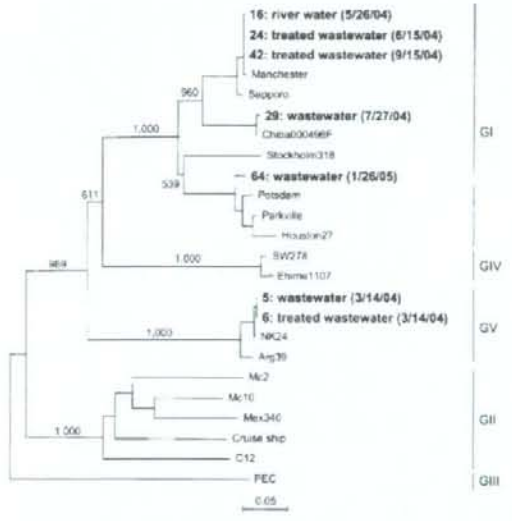

Figure 2. Phylogenetic analysis of sapovirus capsid nucleotide sequence showing different genogroups. Items in **boldface** are sequences isolated in this study and dates of isolation. Numbers on each branch indicate bootstrap values for the genotype. Bootstrap values ≥950 were considered statistically significant for the grouping. The scale bar represents nucleotide substitutions per site. Manchester, X86560; Sapporo, U65427; Chiba000496F, AJ412800; Stockholm318, AF194182; Potsdam, AF294739; Parkville, U73124; Houston27, U95644; SW278, DQ125333; Ehime1107, DQ058829; NK24, AY646856; Arg39, AY289803; Mc2, AY237419; Mc10, AY237420; Mex340, AF435812; cruise ship, AY289804; C12, AY603425; PEC, AF182760.

GV-positive samples were obtained on the same day, although they were obtained from different locations, i.e., untreated wastewater and treated wastewater (Figure 1). Comparison of SaV sequences detected in this study with sequences in GenBank indicated that all 7 isolates closely matched previously reported SaV sequences (Figure 2). Positive SaV samples were obtained in both hot (summer) and cold (winter) months.

Conclusions

Human SaVs infections are being detected more often worldwide (*7,11,12*). These novel results have shown that like NoV (*5*), SaV can also be detected in water samples. Most sequences detected in water samples (5 of 7) belonged to GI. This genogroup likely represents the dominant genogroup worldwide (*7,10,13*). Two sequences (strains 5 and 6) belonged to GV, which has not yet been reported in Japan.

In a similar study, NoV was detected from water samples from the same research locations (*5*). Detection of SaV in river water samples upstream from the wastewater treatment plant suggests human fecal contamination in the river and that SaVs persist in freshwater. Screening for SaV may be worthwhile in oyster samples because NoVs were detected in oysters from local oyster farms (*5*). However, the failure to detect SaV in seawater samples may indicate that the sampling sites were not affected by human fecal contamination or that SaVs do not survive in marine waters. Nevertheless, further environmental studies are clearly needed to address this issue.

This work was supported in part by a grant for Research on Emerging and Re-emerging Infectious Diseases, Research on Food Safety from the Ministry of Health, Labor and Welfare of Japan, and a grant for Research on Health Science Focusing on Drug Innovation from the Japan Health Science Foundation.

Dr Hansman is a scientist at the National Institute of Infectious Diseases in Tokyo, Japan. His research interests include the epidemiology, expression, and cross-reactivity of sapoviruses and noroviruses that cause gastroenteritis in humans.

References

1. Hoebe CJ, Vennema H, Husman AM, van Duynhoven YT. Norovirus outbreak among primary schoolchildren who had played in a recreational water fountain. J Infect Dis. 2004;189:699–705.
2. Brugha R, Vipond IB, Evans MR, Sandifer QD, Roberts RJ, Salmon RL, et al. A community outbreak of food-borne small round-structured virus gastroenteritis caused by a contaminated water supply. Epidemiol Infect. 1999;122:145–54.
3. Cannon RO, Poliner JR, Hirschhorn RB, Rodeheaver DC, Silverman PR, Brown EA, et al. A multistate outbreak of Norwalk virus gastroenteritis associated with consumption of commercial ice. J Infect Dis. 1991;164:860–3.

4. Murphy AM, Grohmann GS, Christopher PJ, Lopez WA, Davey GR, Millsom RH. An Australia-wide outbreak of gastroenteritis from oysters caused by Norwalk virus. Med J Aust. 1979;2:329–33.
5. Ueki Y, Sano D, Watanabe T, Akiyama K, Omura T. Norovirus pathway in water environment estimated by genetic analysis of strains from patients of gastroenteritis, sewage, treated wastewater, river water and oysters. Water Res. 2005;39:4271–80.
6. Katayama H, Shimasaki A, Ohgaki S. Development of a virus concentration method and its application to detection of enterovirus and Norwalk virus from coastal seawater. Appl Environ Microbiol. 2002;68:1033–9.
7. Hansman GS, Takeda N, Katayama K, Tu ET, McIver CJ, Rawlinson WD, et al. Genetic diversity of sapovirus in children, Australia. Emerg Infect Dis. 2006;12:141–3.
8. Okada M, Yamashita Y, Oseto M, Shinozaki K. The detection of human sapoviruses with universal and genogroup-specific primers. Arch Virol. 2006 [Epub ahead of print] PMID number 16847552.
9. Katayama K, Shirato-Horikoshi H, Kojima S, Kageyama T, Oka T, Hoshino F, et al. Phylogenetic analysis of the complete genome of 18 Norwalk-like viruses. Virology. 2002;299:225–39.
10. Hansman GS, Katayama K, Maneekarn N, Peerakome S, Khamrin P, Tonusin S, et al. Genetic diversity of norovirus and sapovirus in hospitalized infants with sporadic cases of acute gastroenteritis in Chiang Mai, Thailand. J Clin Microbiol. 2004;42:1305–7.
11. Johansson PJ, Bergentoft K, Larsson PA, Magnusson G, Widell A, Thorhagen M, et al. A nosocomial sapovirus-associated outbreak of gastroenteritis in adults. Scand J Infect Dis. 2005;37:200–4.
12. Hansman GS, Takeda N, Oka T, Oseto M, Hedlund KO, Katayama K. Intergenogroup recombination in sapoviruses. Emerg Infect Dis. 2005;11:1916–20.
13. Hansman GS, Kuramitsu M, Yoshida H, Katayama K, Takeda N, Ushijima H, et al. Viral gastroenteritis in Mongolian infants. Emerg Infect Dis. 2005;11:180–2.

Address for correspondence: Grant S. Hansman, Department of Virology II, National Institute of Infectious Diseases, 4-7-1 Gakuen, Musashimurayama, Tokyo, 208-0011, Japan; email: ghansman@nih.go.jp

JOURNAL OF VIROLOGY, Nov. 2007, p. 12238–12248
0022-538X/07/$08.00+0 doi:10.1128/JVI.01489-07

Vol. 81, No. 22

Norwalk Virus RNA Is Infectious in Mammalian Cells▽

Susana Guix, Miyuki Asanaka, Kazuhiko Katayama, Sue E. Crawford, Frederick H. Neill, Robert L. Atmar, and Mary K. Estes*

Department of Molecular Virology and Microbiology, Baylor College of Medicine, Houston, Texas 77030

Received 6 July 2007/Accepted 30 August 2007

Human noroviruses are positive-sense RNA viruses and are the leading cause of epidemic acute viral gastroenteritis in developed countries. The absence of an in vitro cell culture model for human norovirus infection has limited the development of effective antivirals and vaccines. Human histo-blood group antigens have been regarded as receptors for norovirus infection, and expression of the α(1,2) fucosyltransferase gene (*FUT2*) responsible for the secretor phenotype is required for susceptibility to Norwalk virus (NV) infection. We report for the first time that transfection of NV RNA, isolated from stool samples from human volunteers, into human hepatoma Huh-7 cells leads to viral replication, with expression of viral antigens, RNA replication, and release of viral particles into the medium. Prior treatment of the RNA with proteinase K completely abolishes RNA infectivity, suggesting a key role of an RNA-protein complex. Although overexpression of the human *FUT2* gene enhances virus binding to cells, it is not sufficient to allow a complete viral infection, and viral spread from NV-transfected cells to naïve cells does not occur. Finally, no differences in NV RNA replication are observed between Huh-7 and Huh-7.5.1 cells, which contain an inactivating mutation in retinoic acid-inducible gene I (RIG-I), suggesting that the RIG-I pathway does not play a role in limiting NV replication. Our results strongly suggest that the block(s) to NV replication in vitro is at the stage of receptor and/or coreceptor binding and/or uncoating, either because cells lack some specific factor or activation of cellular antiviral responses independent of RIG-I inhibits virus replication.

The human pathogen Norwalk virus (NV) is the prototype strain of the *Norovirus* genus in the family *Caliciviridae*. Noroviruses are responsible for the majority of outbreaks of nonbacterial gastroenteritis in developed countries, and it is estimated that they have a significant impact in developing countries as well. Although human noroviruses were originally identified more than 30 years ago, our understanding of their replication cycle and mechanisms of pathogenicity has been limited because these viruses are noncultivatable in established cell lines and a small animal model to study viral infection is not available. Only recently, it has been reported that both genogroup I (GI) and GII strains of human noroviruses can be passaged several times with limited replication in a differentiated three-dimensional cell culture system derived from a human small intestinal cell line (40). In addition, gnotobiotic pigs can support replication of a human norovirus GII strain, with occurrence of mild diarrhea and virus shedding and immunofluorescent detection of both structural and nonstructural proteins in enterocytes (10). Although these results are promising, it remains unclear whether these systems are robust enough to be widely used to efficiently propagate human noroviruses in vitro, and the factors responsible for the block(s) of viral replication using standard cell culture systems remain unknown.

The NV genome is a positive-sense, polyadenylated, single-stranded RNA molecule of 7.7 kb and contains three open reading frames (ORFs): ORF1 encodes a nonstructural polyprotein, and ORF2 and ORF3 encode the major and minor capsid proteins, VP1 and VP2, respectively (14, 24). Due to the lack of an in vitro system to propagate human noroviruses, features of their life cycle have been inferred from studies using other animal caliciviruses that can grow in mammalian cell cultures. A 3′ coterminal polyadenylated subgenomic RNA is produced within infected cells, and it is believed that both genomic and subgenomic RNAs are covalently linked to the nonstructural protein VPg at their 5′ ends. Upon infection of cells, nonstructural proteins are expressed from genomic RNA and form an RNA replication complex, which generates new genomic RNA molecules as well as subgenomic RNAs encoding VP1 and VP2. After expression of the structural proteins from subgenomic RNA molecules, the capsid is assembled and viral RNA encapsidated prior to progeny release. Some of these features have been confirmed using recombinant systems to express the native NV genome in mammalian cells by using vaccinia virus expression systems (2, 25).

Studies with human volunteers have shown that some individuals are either repeatedly susceptible or resistant to NV infection (36) and led to the identification of a genetically determined factor that predicts a person's susceptibility to infection and disease (19, 30). Binding experiments using recombinant NV virus-like particles (VLPs) demonstrated attachment of VLPs to surface epithelial cells of the gastroduodenal junction on biopsies from secretors but not to cells from nonsecretors, showing that the expression pattern of ABH histo-blood group antigens may influence susceptibility to NV (32). The gene responsible for the secretor phenotype encodes an α(1,2)fucosyltransferase (FUT2) that produces H antigens on the surface of epithelial cells and in mucosal secretions (27). Since it was observed that transfection of the *FUT2* gene into nonpermissive cells enhances NV binding (31), it has been

* Corresponding author. Mailing address: Department of Molecular Virology and Microbiology, Baylor College of Medicine, One Baylor Plaza BCM-385, Houston, TX 77030. Phone: (713) 798-3585. Fax: (713) 798-3586. E-mail: mestes@bcm.edu.

▽ Published ahead of print on 12 September 2007.

hypothesized that H antigens or related blood group antigens may function as a receptor for NV.

The main goal of our study was to understand the molecular basis of the restricted growth of NV in cultured cells by transfecting wild-type NV RNA into human cells. Our studies show for the first time that transfection of wild-type NV RNA isolated from human stool samples can lead to the production of viral particles, indicating that wild-type NV RNA is infectious and replicates. However, a block to NV spread to other cells in the culture remains, indicating that the block(s) exists at the cell entry and/or uncoating steps.

MATERIALS AND METHODS

Cell lines and NV stool specimens. The human intestinal CaCo-2 cell line was obtained from the American Type Culture Collection and was maintained in Earle's minimum essential medium (MEM) supplemented with 10% fetal bovine serum (FBS). The hepatic Huh-7 cell line was kindly provided by S. Makino. Huh-7.5.1 cells were kindly provided by F. Chisari (46). Huh-7 and Huh-7.5.1 cells were maintained in Dulbecco's MEM (DMEM) supplemented with 10% FBS.

Stool specimens from human volunteers 715 (100521) and 722 (100619) experimentally infected with NV (A. R. Opekun, R. A. Atmar, M. A. Gilger, M. K. Estes, F. H. Neill, A. Chandrasekaran, C. L. Ugarte, and D. Y. Graham, presented at the Annual Meeting of the American Gastroenterological Association Institute and Digestive Disease Week, 2007; R. Atmar, unpublished data) were used throughout the study. NV titers of stool specimens were higher than 1×10^{11} RNA genomic copies per gram.

Antibodies and plasmids. Polyclonal hyperimmune antiserum to recombinant NV VLPs raised in rabbits and mouse monoclonal antibodies (MAbs) NV3901 and NV8812 have been described elsewhere (16, 23, 35, 43). Antiserum to VPg was made by hyperimmunizing rabbits with a His-tagged VPg expressed and purified in *Escherichia coli* BI-21(DE3) cells. The BG-4 anti-H type 1-specific MAb was purchased from Signet Pathology Systems (Dedham, MA), the BRIC 231 anti-H type 2 MAb was purchased from Biogenesis (United Kingdom), and the anti-Le^b MAb was purchased from Gamma Biologicals (Houston, TX).

An expression vector containing the human secretor blood group *FUT2* gene (accession no. U17894) was kindly provided by John B. Lowe from Case Western Reserve University School of Medicine (27), and pcDNAI (Invitrogen) was used as the corresponding empty vector negative control.

Purification of NV from stool samples. Ten percent stool suspensions in 0.1 M phosphate-buffered saline (PBS)–0.5% Zwittergent detergent (Calbiochem) were extracted with Vertrel XF (Miller-Stephenson) and centrifuged at 12,400 × *g* for 10 min. The supernatant was collected, and virus was precipitated by adding a 3× polyethylene glycol-NaCl (24% polyethylene glycol 8000, 0.12 M NaCl) solution to a final concentration of 1× and incubating the mixture for 2 h at 4°C. The precipitated virus was pelleted at 10,000 × *g* for 15 min, and the pellet was suspended in 0.1 M PBS. The virus suspension was pelleted through a 40% sucrose cushion for 3 h at 124,000 × *g* and further purified by isopycnic CsCl gradient centrifugation in milli-Q water (1.36 g/ml) for 24 h at 150,000 × *g* in a Beckman SW55 Ti rotor. After gradient fractionation, each fraction was diluted 10 times in milli-Q water and viruses were recovered by ultracentrifugation (3 h at 150,000 × *g*). The presence of virus in each fraction was analyzed by enzyme-linked immunosorbent assay (ELISA) specific for the NV VP1 capsid protein as previously described (3), by quantitative real-time reverse transcription-PCR (qRT-PCR) (see below), and by electron microscopy after staining with 1% ammonium molybdate (pH 5.5). Isolation of RNA from the peak fraction containing NV was performed using the QIAamp viral RNA mini kit (QIAGEN) following the manufacturer's instructions.

RNA transfection. Cells were plated into 48-well plates at a density of 5×10^4 cells per well. After incubation overnight at 37°C, cells were washed twice with DMEM containing 2% FBS, and 250 ng of RNA per well was transfected using Lipofectamine 2000 (Invitrogen) following the manufacturer's instructions. In some experiments, Lipofectamine 2000 was used in combination with Magnetofection technology (OZ Biosciences). Briefly, after a 15-min incubation of RNA with Lipofectamine 2000, 1 μl of CombiMag transfection reagent was added to the solution per μg of RNA to be transfected. After a 15-min incubation at room temperature, the mixture was added to each well and cell culture plates were incubated on the magnetic plate for 20 min at 37°C. After a 3-h incubation at 37°C, cells were washed twice with DMEM–2% FBS and incubated in complete media at 37°C for the indicated periods.

Detection of NV proteins in transfected cells by IF analysis. At various hours posttransfection (hpt), cells were rinsed once with 0.1 M PBS and fixed in 4% paraformaldehyde (PF) for 30 min at room temperature. After incubation of cells in 0.5% Triton X-100–0.1 M PBS for 15 min at room temperature for permeabilization, cells were blocked at 37°C for 2 h in 0.1 M PBS–1% bovine serum albumin (BSA). Primary antibodies were added to the wells at the appropriate dilution in 0.1 M PBS–1% BSA (1:1,000 for rabbit anti-VPg and 1:5,000 for MAbs NV3901 and NV8812) and incubated overnight at 4°C. Cells were washed in 0.1 M PBS and incubated for 2 h at room temperature in a 1:1,000 dilution of the corresponding secondary antibody conjugated to Alexa Fluor 594 or 488. Nuclei were stained with 300 nM DAPI (4′,6′-diamidino-2-phenylindole) for 15 min at room temperature. Following the final wash step, immunofluorescence (IF) was detected using an Olympus IX-70 inverted-system microscope.

Proteinase K treatment of NV RNA. Pretreatment of RNA with proteinase K was carried out by incubation of purified RNA in 0.1 M NaCl, 10 mM Tris (pH 8.0), 1 mM EDTA, 0.5% sodium dodecyl sulfate, and 200 μg/ml of proteinase K for 45 min at 55°C followed by precipitation with ethanol. As a control, equivalent amounts of NV RNA were also treated as described above but with the omission of proteinase K.

Northern blotting. RNA samples were loaded onto a denaturing agarose gel for Northern blotting, using the NorthernMax kit (Ambion). Membranes were probed with a negative-sense ^{32}P-labeled RNA probe complementary to nucleotides (nt) 5929 to 6808 of the NV genome. The RNA probe was prepared by in vitro transcription using the Promega Riboprobe in vitro transcription systems, in the presence of 100 μCi of [α-^{32}P]UTP (20 mCi/ml). Genomic and subgenomic RNA controls included RNA transcripts derived from in vitro transcription from the previously described plasmids containing genomic and subgenomic sequences under a T7 promoter (2).

qRT-PCR assay. Two qRT-PCR assays targeted to ORF1 (nt 4641 to 4715) and ORF2 (nt 5412 to 5522) genomic regions were developed. Standard curves or absolute RNA quantification were included in every assay and were generated by using RNA transcripts produced by in vitro transcription of a cDNA that contained both ORF1- and ORF2-targeted regions (nt 4487 to 5671). Primers and probes used to amplify both regions have been previously described (2). Normalization versus glyceraldehyde-3-phosphate dehydrogenase (GAPDH) titers was performed using the TaqMan GAPDH control reagents (human) (Applied Biosystems). Standard curves included five dilutions and three replicate wells for each dilution. All samples were quantified in at least duplicate wells. Reactions were performed using the TaqMan One-Step RT-PCR master mix reagent kit (Applied Biosystems) in an Applied Biosystems 7500 real-time PCR system. The thermal protocol consisted of 30 min at 48°C, followed by 10 min at 95°C and 45 cycles of 15 s at 95°C and 1 min at 60°C.

Analysis of intracellular RNA. Total cellular RNA was isolated from 1×10^5 cells using the RNeasy mini kit (QIAGEN). Poly(A)$^+$ RNA was further purified from total cellular RNA using the MicroPoly(A) Purist kit (Ambion) and analyzed by Northern blotting and qRT-PCR using the same set of primers and probes described above.

Detection of viral RNA, proteins, and viral particles in the culture supernatant of transfected cells. At different hours posttransfection (hpt), the culture supernatants were harvested and clarified at 16,000 × *g* for 15 min at 4°C. NV capsid protein in the supernatant was detected using an ELISA specific for VP1 as previously described (3). For quantification of encapsidated NV RNA, 70 μl of culture supernatant was treated with 20 μg/ml of RNase A for 30 min at 37°C. Viral RNA was purified using the QIAamp viral RNA mini kit (QIAGEN) and subjected to qRT-PCR for ORF1 NV-specific primers. Viral particles were detected by electron microscopy after negative staining with 1% ammonium molybdate (pH 5.5), after concentration of the samples through a 40% sucrose cushion for 3 h at 124,000 × *g*.

Binding assays. Forty-eight hours before performing the binding assay, Huh-7 cells grown on poly-D-lysine-coated 48-well plates were transfected with a plasmid encoding the FUT2 enzyme or the empty vector using Lipofectamine 2000. Both recombinant NV VLPs produced in the baculovirus expression system (43) and wild-type virus isolated from infected human stools were used in binding assays. Cells were washed twice in cold PBS–1% BSA and incubated with 100 μl of 5 μg/ml of VLPs or different doses of purified virus diluted in cold PBS–1% BSA for 1 h at 4°C with gentle agitation. Unbound VLPs or virus were removed by washing three times in cold PBS–1% BSA and two times in cold PBS. To detect VLPs bound to cell monolayers, cells were fixed with 4% PF for 30 min at room temperature and processed for IF as described above, but omitting the permeabilization step, using the MAb NV8812 against VP1 protein. The amount of bound wild-type virus was quantified by qRT-PCR. After the final washing steps, total RNA from each well was isolated using the RNeasy mini kit (QIAGEN) and analyzed by qRT-PCR with NV ORF2 and GAPDH primers.

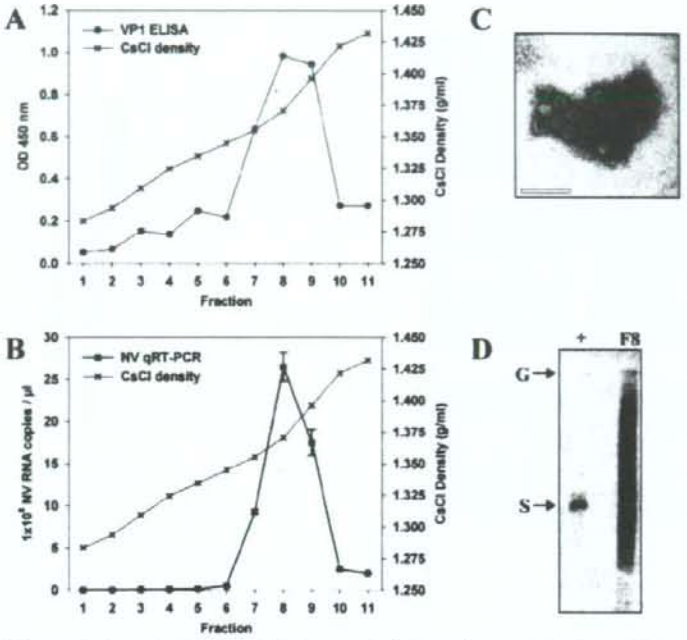

FIG. 1. Purification of NV from stool samples from infected volunteers by CsCl gradient centrifugation. (A) Detection of NV capsid protein VP1 by ELISA in each fraction. (B) Quantification of NV RNA in each fraction by qRT-PCR. (C) Electron micrograph of NV particles after CsCl gradient purification (density, 1.37 g/ml). Scale bar, 100 nm. (D) Northern blot analysis of viral RNA purified from fraction 8 (F8) prior to transfection. In vitro-transcribed positive-sense genomic (G) and subgenomic (S) RNAs were used as positive controls.

The input virus was measured by adding equivalent amounts of virus to wells that had been incubated with PBS–1% BSA alone just before purifying the RNA. Experiments were performed in duplicate wells, and the percentage of bound virus relative to the input virus was calculated after determining the ORF2/GAPDH ratio for each well. The ability of specific MAbs against VP1 to block binding was examined by preincubating the sample in PBS–1% BSA with serial 10-fold dilutions of ascites fluids for 2 h at room temperature as previously described (43), prior to performing the binding assay as described above.

Infection of cultures. Forty-eight hours after transfection of Huh-7 cells grown on 48-well plates with a plasmid encoding the FUT2 enzyme or the empty vector using Lipofectamine 2000, cells were washed twice with serum-free media. The inocula containing wild-type NV isolated from stool diluted in serum-free media was left on the cells for 3 h at 37°C and was replaced with fresh media containing 10% FBS. Cells were fixed with PF at 24 h postinfection (hpi), and viral replication was analyzed by IF using the MAb NV8812 against VP1 protein.

Statistics. All statistical analyses were conducted using the Student's *t* test in SigmaPlot 10.0. Error bars represent standard deviation, and statistical significance was defined as $P < 0.01$.

RESULTS

Isolation of NV RNA from human stool samples. Stools from two volunteers containing high titers of NV were used as a source of wild-type NV RNA. Virus was purified from 5-g aliquots of stool by CsCl gradient centrifugation, and each fraction was suspended in a final volume of 100 µl of milli-Q water. The presence of VP1 antigen and NV RNA in each fraction was analyzed by ELISA (Fig. 1A) and qRT-PCR (Fig. 1B). The peak viral antigen and nucleic acid corresponded to fractions with CsCl densities of 1.37 to 1.39 g/ml, which is consistent with previous reports for noroviruses (22). The presence of viral particles in these fractions was confirmed by electron microscopy (Fig. 1C). NV RNA was purified from 15 µl of the peak fraction (fraction 8), and the RNA integrity was assessed by Northern blotting before transfection (Fig. 1D), showing a major band of 7.7 kb corresponding to the size of NV genomic RNA.

Transfection of wild-type NV RNA into CaCo-2 and Huh-7 cells leads to expression of viral antigens. Since it is believed that the NV RNA 5′ end is covalently linked to a VPg protein, proteinase K was not used to extract the RNA from NV particles purified from stool. NV wild-type RNA was purified from CsCl fractions using the QIAamp viral RNA mini kit (QIAGEN), which is based on the binding properties of nucleic acids to a silica gel-based membrane, in the presence of carrier RNA. Purified RNA used for transfection had a concentration of 70 ng/µl, containing between 1×10^8 and 1×10^9 NV RNA molecules/µl. When 250 ng of purified viral RNA was used to transfect cells of the human intestinal cell line CaCo-2 and human hepatoma cell line Huh-7 grown on 48-well plates, expression of both nonstructural and structural proteins was observed in both cell lines at 48 h after transfection, using antiserum against VPg and the MAb NV3901 against VP1 protein, respectively (Fig. 2). Although the number of positive cells was low in all cases, Huh-7 cells showed the highest ratio of transfected cells/copy of transfected NV RNA. Around 100 to 150 positive cells could be detected after transfecting 5×10^8 NV RNA molecules in 1×10^5 cells. Other cell lines such

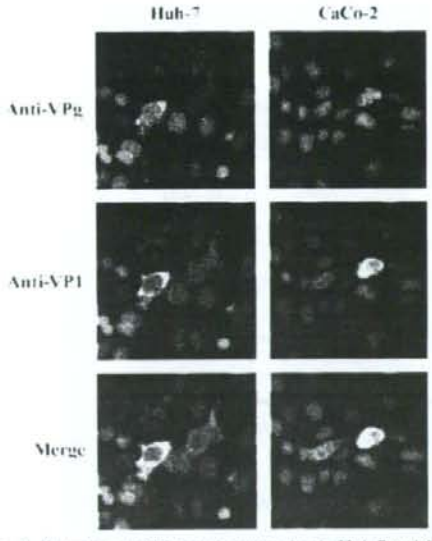

FIG. 2. Detection of NV protein expression in Huh-7 and CaCo-2 RNA-transfected cells at 48 hpt. Immunofluorescent staining for nonstructural proteins was performed using antiserum against the VPg protein. Capsid protein VP1 was stained with the MAb NV3901. Nuclei were counterstained with DAPI.

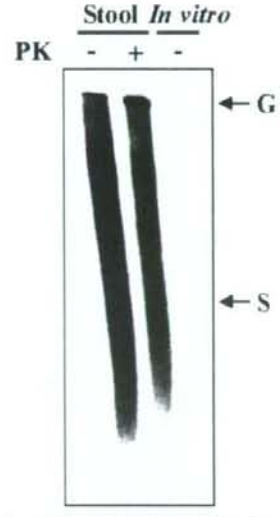

FIG. 3. Northern blot analysis of equal amounts of NV RNA isolated from stool after treatment in the presence (+) or absence (−) of proteinase K (PK). In vitro-transcribed positive-sense genomic (G) and subgenomic (S) RNAs without PK treatment were used as positive controls.

as Int407 and HEK293T cells also supported NV protein expression after RNA transfection, but the ratios of transfected cells per copy of transfected NV RNA were lower than that for Huh-7 cells (data not shown). Since capsid proteins are translated from subgenomic RNA, detection of both structural and nonstructural proteins indicated that transfected NV RNA was able to replicate and that synthesis of subgenomic RNA occurred.

Expression of viral RNA is likely dependent on VPg linkage to genomic RNA. To further analyze the infectious properties of wild-type NV RNA, RNA isolated from stool was treated with or without proteinase K. Prior to transfection, integrity of RNA was confirmed by Northern blotting (Fig. 3) and qRT-PCR. As measured by qRT-PCR with primers targeted to the ORF2 region, the titers of NV RNA in the absence and presence of proteinase K treatment were similar [$(2.05 \pm 0.01) \times 10^7$ and $(3.54 \pm 0.12) \times 10^7$ NV RNA copies/ng of RNA, respectively]. The number of positive cells after transfection of equal amounts of RNA in Huh-7 cells was evaluated by IF staining using antibodies against VPg and MAb NV8812 at 24 h after transfection with 250 ng of RNA in Huh-7 cells grown on 48-well plates. While in the absence of proteinase K treatment 10^5 cells expressed VP1 protein, proteinase K treatment completely abolished viral expression, suggesting that NV viral protein expression is dependent on an RNA-protein interaction.

NV RNA transfection leads to a single cycle of viral replication. A kinetic analysis of NV protein expression in Huh-7 cells showed that although clusters containing four to six positive cells were frequently observed by 2 days posttransfection (dpt), a significant increase in the percentage of positive cells over time was not detected, and morphological changes were observed by 4 dpt (Fig. 4A). Morphological changes observed in NV-expressing cells are analyzed in more detail at higher magnification in Fig. 4B. Between 2 and 3 dpt, NV-transfected cells started to detach from the plate surface, and by 5 dpt, the vast majority of NV-transfected cells showed dramatic cytopathic effects that resulted in cell lysis. Altogether, these results suggest that cell-to-cell spread of virus resulting in infection of the complete cell monolayer did not occur. Next, to elucidate whether a complete cycle of viral replication occurred, we tested whether different steps of the viral replication cycle, such as viral RNA replication and assembly and release of progeny virus to the media, could be observed.

Poly(A)-containing RNA produced in Huh-7-transfected cells at different times posttransfection was examined by Northern blot analysis, using an antisense RNA probe specific for the NV ORF2 region and qRT-PCR using primers targeting regions either in ORF1 or ORF2. While ORF2 primers are able to amplify both genomic and subgenomic RNAs, ORF1 primers will only amplify genomic RNA. By Northern blotting, a band corresponding to positive-sense subgenomic RNA was detected starting at 24 hpt. A clear band corresponding to genomic RNA could not be observed, probably due to the low number of NV-transfected cells and low sensitivity of Northern blots, especially to detect high-molecular-weight bands (Fig. 5A). By qRT-PCR, however, an increase in RNA templates amplified by both ORF1 and ORF2 primers began to be observed at 24 hpt and was more obvious at 48 hpt (Fig. 5B). Although at 0 hpt, the titer using ORF2 primers was approximately 3 times lower than the titer obtained with ORF1 primers, probably due to different primer sensitivities, increases of 9-fold and 31-fold were observed from 0 to 48 hpt for ORF1

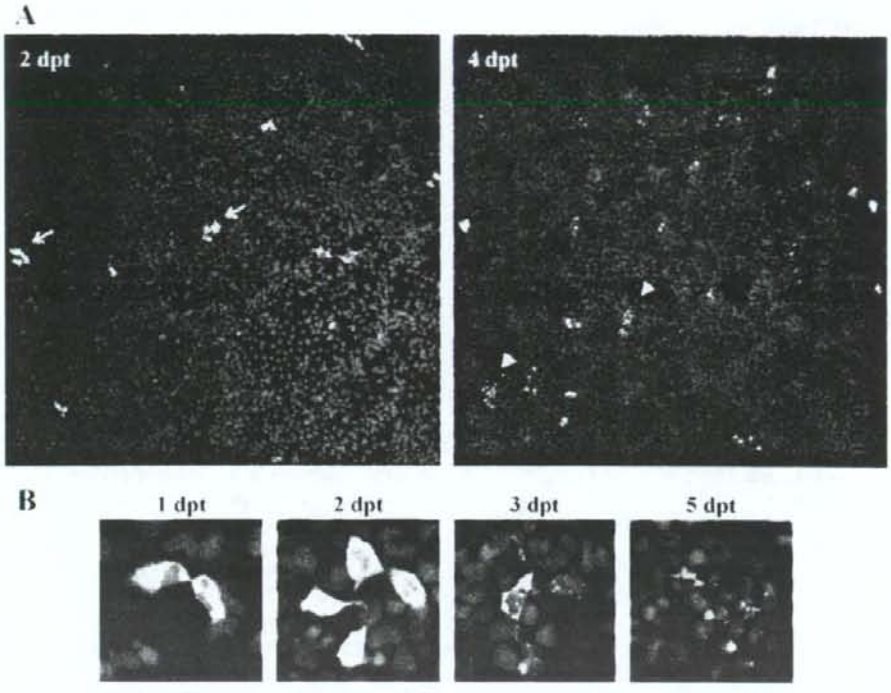

FIG. 4. Time course analysis of NV capsid protein expression by IF staining in transfected Huh-7 cells. (A) NV RNA-transfected Huh-7 cells at 2 and 4 dpt. Magnification, ×40. Arrows indicate clusters of four to six transfected cells, and arrowheads indicate lysed cells. (B) Analysis of changes in Huh-7 cell morphology over time after NV RNA transfection. Magnification, ×200.

and ORF2 primers, respectively, indicating that both genomic and subgenomic RNAs were being synthesized. Levels of GAPDH mRNA did not change. The higher increase (fold) detected with ORF2 primers indicated that subgenomic RNA was being synthesized and confirmed the results obtained by Northern blotting. The larger amounts of subgenomic RNA molecules compared to genomic RNA molecules are expected, since similar results are seen during replication of other positive-strand RNA viruses that use subgenomic RNA to synthesize large amounts of capsid proteins, such as togavirus (38) or astrovirus (33).

To determine whether viral particles were generated and released from cells, the presence of viral RNA and VP1 protein in the culture supernatant was confirmed by qRT-PCR and ELISA, respectively (Fig. 6A). To rule out the detection of input or free viral RNA, culture supernatants were treated with RNase A prior to extraction of RNA. Overall, a 3-$\log_{10}$ increase in viral RNA was detected from 0 h to 96 hpt, reaching a titer of $(1.4 \pm 0.4) \times 10^7$ NV RNA copies/ml. A correlation was observed in the detection of viral protein by ELISA and RNA titer, and intact virions were detected by electron microscopy in samples concentrated by pelleting through a sucrose cushion (Fig. 6B). Taking into account the number of positive cells detected by IF at 24 hpt in each transfected well, it was possible to estimate that at 96 hpt, each NV-transfected cell had released approximately $(2.8 \pm 0.8) \times 10^4$ genome-containing virions. Finally, biophysical properties of released virions were examined by subjecting the concentrated culture supernatants to isopycnic CsCl gradient centrifugation. The presence of encapsidated viral RNA in each CsCl fraction was analyzed by qRT-PCR. Prior to RNA extraction, each fraction was treated with RNase A to avoid the detection of free viral RNA. A peak of NV RNA was detected at a density of 1.37 g/ml (Fig. 6C), which is similar to that of wild-type virions isolated from human stool samples. Studies to analyze whether RNA extracted from released virus was also infectious were not possible due to the insufficient amount of NV RNA isolated from these particles. While a minimum concentration of 5×10^7 NV RNA copies/μl of purified stool sample was required to detect positive transfected cells by IF, the amount of virus particles released into the supernatant after RNA transfection was not higher than 1×10^4 NV RNA copies/μl.

Taken together, our results indicate that NV RNA isolated from infected stools is infectious and can produce virions when transfected into Huh-7 cells. However, since a significant increase in the percentage of positive cells was not observed over time by IF, NV RNA transfection most likely leads to a single cycle of viral replication, and released virions are not able to infect new cells. Failure to infect new Huh-7 cultures using either wild-type virus isolated from stool or virus produced by NV RNA transfection confirmed these observations (data not shown).

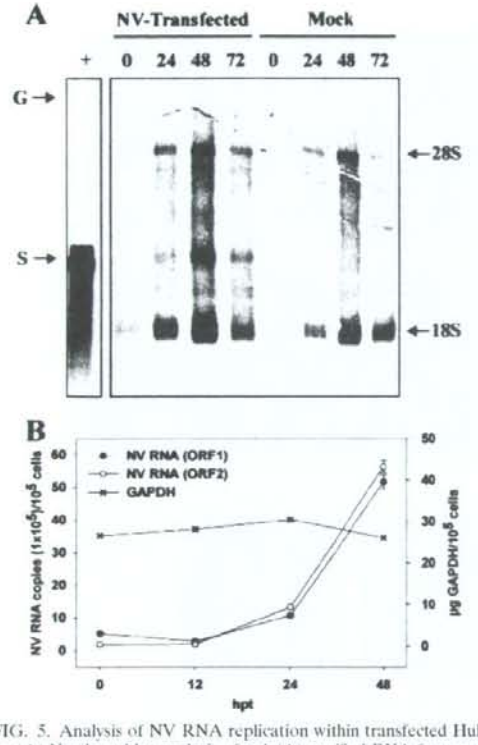

FIG. 5. Analysis of NV RNA replication within transfected Huh-7 cells. (A) Northern blot analysis of poly(A)-purified RNA from transfected cells using a negative-strand RNA probe targeting the ORF2 region at different hours posttransfection (hpt). In vitro-transcribed positive-sense genomic (G) and subgenomic (S) RNAs were used as positive controls. Nonspecific bands corresponding to 28S and 18S ribosomal RNAs are indicated. (B) Levels of NV RNA in poly(A)-purified RNA from transfected cells were measured by qRT-PCR using primers against ORF1 and ORF2 regions and GAPDH.

Overexpression of the human FUT2 gene in Huh-7 cells enhances virus binding but does not lead to viral infection. Since expression of certain H antigens is required for susceptibility to NV infection, we wanted to analyze whether Huh-7 cells express histo-blood group antigens on the cell surface. A phenotyping assay for the expression of some of the main carbohydrate antigens previously shown to be involved in NV binding (H type 1, H type 2, and Le^b) was performed on Huh-7 cells. Differentiated CaCo-2 cells (D-CaCo-2) were used as a positive control. Confluent cell monolayers fixed with PF were tested for histo-blood group antigen expression on the cell surface by IF, omitting the permeabilization step. The results indicated that while D-CaCo-2 cells express high levels of H type 1, H type 2, and Le^b carbohydrates (Fig. 7, A to C), only a low percentage of Huh-7 cells express levels of Le^b antigen detected by IF staining (Fig. 7D to F).

In case the expression level of histo-blood group antigens on Huh-7 cells was not sufficient to support NV binding and entry, and to enhance expression of the putative NV receptor, Huh-7 cells were transfected with a plasmid encoding the human secretor blood group $\alpha(1,2)$ fucosyltransferase (FUT2). Transient expression of FUT2 in these cells resulted in a significant increase in Le^b antigen expression at 48 hpt, but we did not observe an increase in the levels of H type 1 or H type 2, at least not up to levels detectable by IF with the available antibodies (Fig. 7G to I).

Binding assays using recombinant NV VLPs and NV purified from stool were performed with Huh-7 cells transfected with either the *FUT2* plasmid or pcDNAI empty vector as a negative control and showed that FUT2 transient expression significantly enhanced NV and VLP binding. IF analysis using MAb NV8812 showed that the VP1 protein of VLPs could be detected on the surface of cells (Fig. 8A). Table 1 shows the percentage of bound virus after incubating *FUT2*- and pcDNAI-transfected cultures with three different doses of wild-type NV virus purified from stool. Bound virus was quantified by qRT-PCR and normalized versus the number of cells with measurements of GAPDH mRNA levels. While less than 1% of the input virus bound to Huh-7 cells transfected with the empty vector, significantly more virus (up to 16.6%) bound to Huh-7 cells transfected with the *FUT2* gene.

Due to the limited amounts of NV that can be isolated from stool samples, it was not possible to analyze whether NV binding to FUT2-expressing Huh-7 was saturable. However, specificity of the virus binding was examined by preincubating the virus with serial dilutions of ascites fluids with MAbs NV8812 and NV3901. MAb NV8812 recognizes a conformational

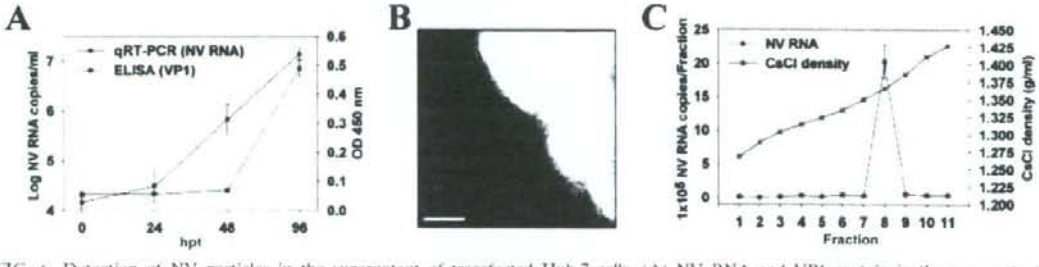

FIG. 6. Detection of NV particles in the supernatant of transfected Huh-7 cells. (A) NV RNA and VP1 protein in the supernatant of transfected cultures over time were measured by qRT-PCR using ORF1 primers and ELISA, respectively. (B) Electron micrograph of viral particles released into the supernatant after a concentration step by sucrose cushion. Scale bar, 50 nm. (C) Analysis of biophysical properties of released particles by CsCl density gradient. The titer of NV RNA in each CsCl fraction was measured by qRT-PCR using ORF1 primers.

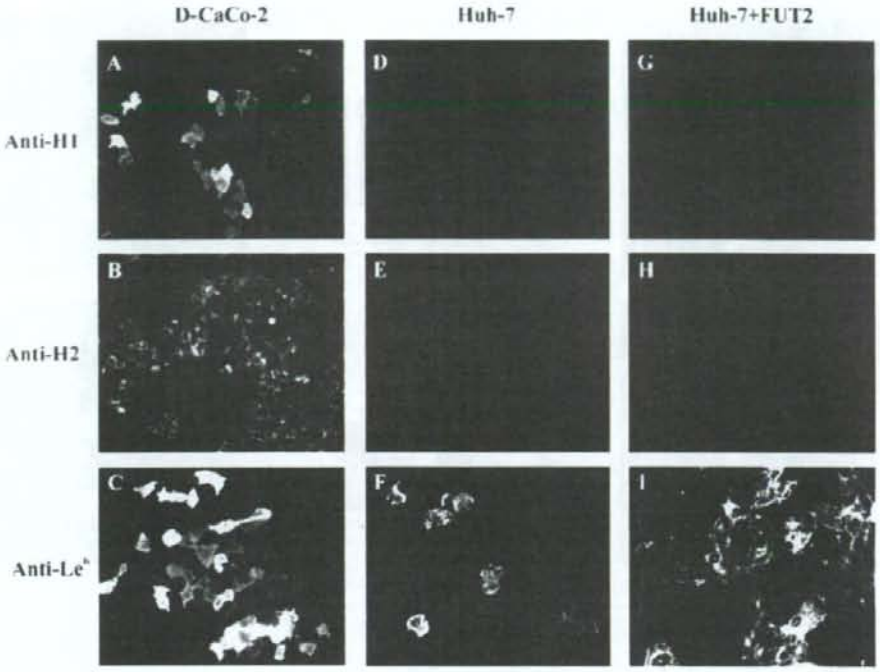

FIG. 7. Histo-blood group antigen phenotyping by IF assay on differentiated CaCo-2 cells (D-CaCo-2) (A to C), Huh-7 cells (D to F), and Huh-7 cells overexpressing the human FUT2 gene (48 hpt) (G to I). Antibodies against the H type 1, H type 2, and Le^b carbohydrates were used to detect carbohydrates.

epitope in the P2 protruding domain of VP1 and was previously shown to block binding of NV VLPs to D-CaCo-2 cells (43), as well as to inhibit hemagglutination of red blood cells by NV VLPs (21). MAb NV3901, a GI-cross-reactive MAb that recognizes an epitope within the C-terminal P1 subdomain of VP1 (35) and does not have any effect on NV VLP binding to D-CaCo-2 cells, was used as a negative control. While MAb NV3901 had no effect on NV binding, MAb NV8812 was able to block NV binding in a dose-dependent manner (Fig. 8B). These results confirm that attachment of both NV VLPs and wild-type virus to cells requires expression of FUT2 and is mediated by recognition of a histo-blood group H-related antigen by some residues of the P2 protruding domain of VP1 protein.

Cotransfection of NV wild-type RNA with FUT2 expression plasmid does not enhance released virus spreading to neighboring cells. Since FUT2 overexpression increased the amount of NV binding, we next asked whether cells overexpressing FUT2 would support a productive NV infection following NV RNA transfection or NV infection. To examine whether transfection of NV RNA in FUT2-expressing cells would result in a productive NV infection of the cell monolayer with virus spreading from initially transfected cells to naïve cells, NV RNA from stool was purified using the QIAamp viral RNA mini kit (QIAGEN), adding either pcDNAI or *FUT2* plasmids instead of carrier RNA to lysis buffer AVL, and transfected into Huh-7 cells. Ninety-six hours after transfection of samples in triplicate wells, IF staining for Le^b carbohydrate was performed in one well to monitor efficiency of FUT2 expression, and IF staining for NV capsid protein was performed in the remaining two wells to count the number of NV-transfected cells per well. NV RNA in the media of each well was quantified by qRT-PCR using NV primers targeted to ORF1 region, and virus yields were compared between NV RNA-pcDNAI- and NV RNA-*FUT2*-transfected wells. No statistically significant differences were detected either in the number of VP1-positive cells counted by IF (data not shown) nor in the virus yield measured in the supernatant by qRT-PCR (Fig. 8C), indicating that overexpression of FUT2 did not result in virus spreading through the cell culture. Although differences in virus yield were not statistically significant ($P < 0.01$), the NV titer detected in the supernatant of NV RNA-*FUT2*-transfected cells was 0.2 log lower than in NV RNA-pcDNAI-transfected cells (Fig. 8C). Since overexpression of FUT2 induced an increase in virus binding to cells, virus yield measured in the supernatant of NV RNA-*FUT2*-transfected cells may have been lower due to the binding of a portion of the released viruses to the remaining uninfected cells on the monolayer.

In an alternative approach, 48 h after transfection of Huh-7 cells with the *FUT2* plasmid or the empty vector, cultures were infected with wild-type NV virions isolated from stool, using a multiplicity of infection of 7×10^8 NV RNA copies/1×10^5 cells. Results of IF staining using the MAb NV8812 against VP1 protein performed at 24 hpi showed that bound virus was

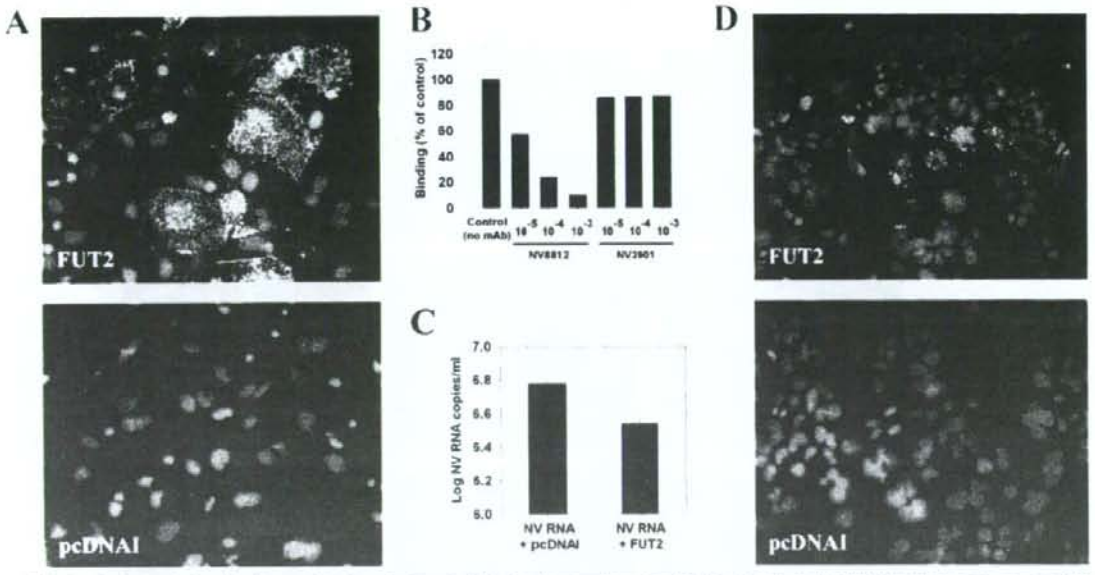

FIG. 8. Analysis of virus binding and viral replication in Huh-7 cells overexpressing FUT2. (A) Effect of FUT2 transient expression on NV binding to Huh-7 cells. Huh-7 cells were transfected with a plasmid carrying the human *FUT2* gene or the empty vector (pcDNAI), and 48 hpt, binding assays were performed. Binding of recombinant NV VLPs (5 μg/ml) to Huh-7 cells was detected by IF using the MAb NV8812. (B) Effect of MAbs against NV VP1 on the binding of wild-type NV to FUT2-expressing Huh-7 cells. Purified NV from stool was incubated in three serial 10-fold dilutions of ascites fluids from MAbs NV8812 and NV3901, starting at a 10^{-3} dilution, for 2 h at room temperature before performing the binding assay. A dose of 2×10^7 NV RNA copies/1×10^5 cells was used. Bound virus was measured by qRT-PCR and normalized versus the number of cells by measurements of GAPDH mRNA levels. Results are expressed as percentage of the control (absence of MAb). The data plotted represent the means of duplicate wells. (C) Quantification of the NV virus yield in the supernatant of cultures cotransfected with NV RNA plus pcDNAI and NV RNA plus *FUT2* by qRT-PCR at 96 hpt. The data plotted represent the means ± standard deviation of triplicate wells. (D) Infection of Huh-7 cells transfected with the empty vector (pcDNAI) or the *FUT2* plasmid, and detection of VP1 protein by IF at 24 hpi using MAb NV8812. DAPI was used for nuclear counterstaining.

only detected on Huh-7 cells that expressed FUT2 (Fig. 8D). No expression of nonstructural proteins was detected (data not shown). Although VP1 of bound virus could still be detected 72 hpi, no viral replication occurred. These results indicated that although FUT2 expression increased binding, cells were not permissive to infection, either due to the lack of a factor required during viral entry and/or uncoating or due to the induction of a cellular response that would inhibit replication.

Inactivation of RIG-I does not affect NV RNA replication. Recent studies have suggested that cellular innate immune responses play an important role in the control of norovirus replication (7, 44). To examine whether NV RNA replication could be enhanced by suppressing innate immunity, we compared the abilities of the Huh-7 and Huh-7.5.1 cell lines to replicate and produce NV. Huh-7.5.1 cells were derived from the parental Huh-7 cells that harbored a subgenomic hepatitis C virus (HCV) replicon, after curing them by prolonged treatment with alpha interferon (IFN-α). These cells are deficient in virus-activated signaling of IFN-β synthesis through the intracellular retinoic acid-inducible gene I (RIG-I) pathway and are highly permissive for HCV replication (4, 41). To determine whether there were quantitative differences in replication efficiencies between Huh-7 and Huh-7.5.1 cells, equal amounts of NV RNA were transfected in both cell lines in parallel, and kinetics of viral replication were compared after quantifying the released virus in the supernatant at different times posttransfection. The numbers of positive cells by IF at 24 hpt were similar for both cell lines, indicating that RNA transfection efficiencies were similar for both cell lines. NV particle release into the supernatant of transfected Huh-7 cells was slightly delayed compared to production by Huh-7.5.1 cells (Fig. 9), but the differences were not statistically significant. Similar levels of intracellular synthesized subgenomic RNA were detected by Northern blotting between both cell lines (data not shown). These results demonstrate that NV RNA replication efficiencies are similar between Huh-7 and Huh-7.5.1 cells and suggest that an inactivating mutation in RIG-I does not have any effect on NV RNA replication and that the RIG-I signaling

TABLE 1. Percentage of NV bound to Huh-7 cells transfected with pcDNAI or the *FUT2* gene

Amt of input virus (NV RNA copies/ 1×10^5 cells)	% of virus bound	
	Empty vector (pcDNAI)	*FUT2*
1.4×10^7	0.58 ± 0.08	10.99 ± 0.48
7.0×10^7	0.97 ± 0.13	9.91 ± 1.00
3.4×10^8	0.93 ± 0.08	16.64 ± 3.44

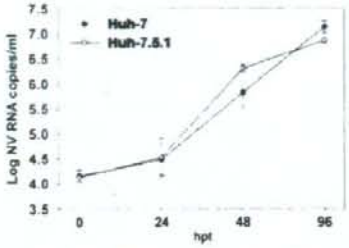

FIG. 9. Kinetics of NV infection in Huh-7 and Huh-7.5.1 cells after RNA transfection. Equal amounts of purified NV RNA were used to transfect Huh-7 and Huh-7.5.1 cells. Released virus in the supernatant was measured by qRT-PCR at the indicated times posttransfection. The data plotted represent the means ± standard deviation of triplicate wells.

pathway does not account for the block to NV infection in Huh-7 cells.

DISCUSSION

The absence of a robust cell culture model for NV infection has limited the study of the NV life cycle, development of effective antivirals and vaccines, and determination of correlates of protection for infection. Here we report for the first time that NV RNA isolated from stool from human volunteers is fully infectious in cultured human cells. Transfection of NV RNA into human hepatoma cells leads to expression of viral antigens and viral replication, with release of viral particles into the medium. These results provide useful information for understanding the block(s) in NV replication in cell culture, since they demonstrate that once NV RNA is introduced into Huh-7 cells, viral replication and viral progeny release occur unhindered. Thus, a lack of a host factor involved in intracellular expression and replication of the viral genome does not seem to be the cause of restriction for virus replication.

Since Huh-7 cells were isolated from a human hepatocarcinoma (34), the high susceptibility of these cells to NV replication initially was unexpected. However, our results are consistent with data published by Chang et al. (7), which show that Huh-7 cells can harbor a NV RNA replicon, suggesting that these cells are highly susceptible to NV replication. Not only have Huh-7 cells been very successful in allowing replication of other fastidious gastrointestinal viruses such as HCV (29, 42, 45, 46) and hepatitis A virus (28), but they have also been shown to support growth of many respiratory RNA viruses (11).

Since translation and infectivity of RNA purified from infected cells or virions of other caliciviruses are drastically reduced by treatment of RNA with proteinase K (5, 8), we examined the effect of this enzyme on wild-type NV RNA. Prior treatment of the RNA with proteinase K completely abolished protein expression after transfection, suggesting that the covalent linkage of RNA to a protein, likely VPg, plays an important role in infectivity and expression of the NV genome, similar to animal caliciviruses (8, 15, 17, 39). Our attempts to recover viral particles by transfecting cells with capped in vitro-transcribed RNA from a full-length NV genomic cDNA have been unsuccessful (data not shown). Although norovirus genome replication and packaging by mammalian cells have been recently demonstrated using different recombinant vaccinia virus expression systems (2, 25), the low efficiency of these systems has not allowed the visualization of recovered virus particles with calicivirus morphology. Since neither of these reverse genetics systems has determined whether VPg was covalently attached to the 5′ end of generated genomic and subgenomic RNAs, the low efficiency of these systems may be explained in part by the fact that a high percentage of the transcripts produced by T7 RNA polymerase in vaccinia virus-infected cells are not linked to a VPg protein but to a cap structure (12).

Demonstrating that human NV RNA is infectious when transfected into cells potentially has important implications. First, although the amount of NV RNA that can be isolated from human stools is limited, the ability to monitor wild-type NV RNA expression and replication in human cells can be used to test the effect of antivirals on NV replication and will help to provide more insights into the NV life cycle, such as the characterization of the RNA replication sites within the cell or the molecular basis of cell death after infection, and proteins involved in these key pathways may become new targets for development of antivirals. Second, since most current methods to detect noroviruses are based on detection of viral nucleic acid by RT-PCR, it is not possible to know whether detected virus is truly infectious or not and whether it represents a potential risk for virus transmission. Until a robust cell culture system is widely available to grow human noroviruses, testing of infectivity by RNA transfection may provide additional information about the infectious capacity of a potentially contaminated sample. However, methods to increase NV RNA isolation from different kinds of samples and transfection efficiency will be required, as currently large amounts of viral RNA are needed to detect replication. Since a certain level of denaturation of the RNA-linked VPg protein may occur with the use of guanidine salts in the RNA purification process, and this could partially account for the low number of positive cells after transfection, the use of other RNA extraction methods might improve the efficiency of the RNA infectivity assays.

Previous work showed that transfection of cells with fucosyltransferases can enable recombinant NV VLP binding. This was achieved with Chinese hamster ovary (CHO) cells, which normally do not express H antigen carbohydrates and show little binding to VLPs. When these cells were transfected with the rat homologue of the human *FUT2* gene, they expressed H type 1 and bound NV VLPs (31). Our current work demonstrates that the lack of carbohydrate expression does not explain the block to NV replication. For example, CaCo-2 cells are a human intestinal cell line derived from a secretor-positive individual of blood type O and these cells express the H antigen (1) and show the best binding to NV VLPs (43). Although these cells can replicate wild-type NV RNA and express capsid proteins after transfection, infection does not spread cell to cell over time. Our results indicate that if receptor binding, internalization, and uncoating steps are circumvented, these cells can fully replicate the viral RNA. Unfortunately, due to the low transfection efficiency observed with this cell line, we were unable to confirm the presence of released virions from RNA-transfected CaCo-2 cells, and the possibility that these cells